THE AMERICAN MINERALOGIST

JOURNAL OF THE MINERALOGICAL SOCIETY OF AMERICA

Vol. 26 DECEMBER, 1941 No. 12

CHEMICAL COMPOSITION AND GENESIS OF GLAUCONITE AND CELADONITE*

Sterling B. Hendricks, *U. S. Bureau of Plant Industry*,

AND

Clarence S. Ross, *U. S. Geological Survey*.

Abstract

A method of study found applicable to the clay minerals clarifies the chemical relations of glauconite and celadonite, and gives significant information about their genesis.

The representative formula of glauconite is:

$$(K, Ca_{\frac{1}{2}}, Na)_{.84}(Al_{.47}Fe'''_{.97}Fe''_{.19}Mg_{.40})(Si_{3.65}Al_{.35})O_{10}(OH)_2$$

and of celadonite is:

$$(K, Ca_{\frac{1}{2}}, Na)_{.84}(Al_{.34}Fe'''_{.76}Fe''_{.24}Mg_{.76})(Si_{3.89}Al_{.11})O_{10}(OH)_2,$$

which represent very closely compositions of a large number of mineral specimens. These formulas show that both minerals belong to the heptaphyllite group of micas.

A supply of ferrous iron (necessitating a reducing environment), magnesium, and potassium, is a controlling condition for the formation of both minerals. Glauconite, which forms only in a marine environment, maintained in a reducing condition by bacterial action, derives its magnesium and potassium from the sea water, and its other constituents from mud. Celadonite, which commonly forms in vesicular basalts, derives its essential magnesium, iron, and silica from olivine, and its other constituents from deuteric solutions.

Introduction

In the course of work on the montmorillonite-nontronite group of clay minerals it became evident that the methods used in correlating chemical analyses of that group might give interesting information on other minerals related to the micas. Glauconite being a mica is a mineral of this type, and its widespread occurrence has caused it to be the subject of many studies. Glauconite has formed as a marine deposit in every geological age since the pre-Cambrian and is found in many modern marine sediments. A material known as celadonite that occurs as vesicular fillings in basaltic rocks, has been correlated with glauconite.[1,2] Glauconite has been identified as a mica by several investigators,[3,4,5,6,7] and celadonite, although less widely investigated,has been assigned to the micas by Glinka and this has been verified by Maegdefrau and Hofmann[8] using x-ray diffraction methods, and confirmed by our own observations.

---

* Approved for publication by the Chief of Bureau of Plant Industry and Director of U. S. Geological Survey.

[1] Lacroix, A., *Mineralogie de la France et de ses Colonies*, **1**, part 1, 406–409 (1893).

[2] Glinka, K., Der Glauconite, sein Entstehung, sein chemischer Bestand, und die Art und Weise seiner Verwiterung: *Pub. de l'Institut agromique de Novo. Alex Russie, St. Petersberg* (**1896**).

These calculations of the chemical relations of glauconite and celadonite are based on the assumption that there are no major analytical errors in the analyses, and that the material analyzed was fairly free from impurities. It is believed that the consideration of an adequate number of analyses will obviate the difficulty introduced by minor errors and that major ones will become self evident. The method of consideration is based on the establishment of a consistent trend in composition that agrees with crystal structure, and recognized ionic substitutions. Measured by these criteria, the available analyses seem to give a consistent picture; in fact, the departures from this trend are less important than were to be expected.

Mode of Occurrence and Physical Ppoperties

Glauconite as it occurs in sedimentary rocks is so well known and has been so often described that little need be said about its occurrence and properties.

Sedimentary glauconite most commonly occurs as rounded pellets from one to several millimeters in diameter, its formation by replacement of foraminifera being on the whole exceptional. It is commonly made up of an exceedingly fine-grained, but obviously crystalline aggregate of overlapping crystal plates. However, almost all who have investigated glauconite[9,10,11,12,13,14,15] have found grains that were crystal units.

---

[3] Murray, Sir John, *Challenger Rept., Deep sea deposits*, 239 (**1891**).

[4] Lacroix, A., *op. cit.*

[5] Glinka, K., *op. cit.*

[6] Schneider, H., A study of glauconite: *Jour. Geol.*, **35**, 289–310 (1927).

[7] Gruner, John W., The structural relationship of glauconite and mica: *Am. Mineral.*, **20**, 699–714 (1935).

[8] Maegdefrau, E., and Hofmann, U., Glimmerartige Mineralien als Tonsubstanzen: *Zeits. Krist.*, **A98**, 31–59 (1937).

[9] Lacroix, A., *op. cit.*

[10] Cayeux, L., *Contribution a l'etude des Terrains Sedimentaires, Lille*, 163–164 (**1897**).

[11] Mansfield, G. R., Potash in the greensands of New Jersey: *U. S. Geol. Surv., Bull.* **727**, Plate, 4D (1922).

[12] Hadding, A., The pre-Quaternary sedimentary rocks of Sweden. IV. Glauconite and glauconitic rocks: *Medd. Lunds Geol.-Mineral Institute*, **51**, 51 (1932).

[13] Ross, Clarence S., The optical properties and chemical composition of glauconite: *Proc. U. S. Nat. Museum*, No. 2628, **69**, 1–15 (1926).

[14] Schneider, Hyrum, *op. cit.*

[15] Ichimura, T., Some glauconitic rocks from Taiwan (Formosa): *Memoirs Faculty Science and Agri., Taihoku Imperial Univ.*, **22**, No. 3, 25–63, plate 4 (1940).

Some of these are roughly hexagonal in outline, and Lacroix, Cayeux, and Ross, found evidence of a small inclination of the optic axis, thus indicating monoclinic symmetry. The optical properties reported agree within fairly narrow limits and those determined (Table 1) on the unusually good material from Bonne Terre, Missouri,[16] are adequately representative.

The properties of celadonite have not been determined as fully as have those of sedimentary glauconite, and so the occurrence and properties will be described in the following section.

The name celadonite was proposed by Glocker[17] in 1847, although the same material had been previously described as terra verte[18] and grünerde.[19] Celadonite is most abundant in vesicular cavities in basalt; but it also replaces olivine, and less commonly hypersthene or groundmass material. It forms radial or vermicular aggregates that have commonly been described as fibrous, but detailed study indicates that it is made up of minute elongated plates, and that the habit is bladed. In hand specimens the appearance is earthy, but in good light reflections from minute crystal faces may be observed. The color is commonly blue-green in the hand specimen, and under the microscope the material commonly has a decided blue cast in the direction of maximum absorption, and is yellow, yellow-green, or pale green in the other direction. The mode of occurrence of representative samples of the celadonite are as follows:

The material from Reno, Nevada, occurs as vesicular fillings in a fine-grained olivine basalt. The olivine has locally been partly altered to the same material, but in general there has been complete alteration to serpentine. The filled vesicular cavities in the basalt vary in size up to a diameter of 12 millimeters, and thus are unusually large. The color of the compact material is light Danube green (Ridgway) and the powdered material Montpelier green. Most of the cavities are completely filled with celadonite, but a few are hollow or contain irregular areas of iron-rich saponite (as shown in Plate 1, Fig. *d*). A few of the smallest cavities contain only saponite.

The material from Sandoval County, New Mexico (collected by B. C. Renick), a photomicrograph of which is shown as Plate 1, Fig. c, fills more or less irregular or flattened vesicular cavities that reach a maximum length of 10 millimeters. The color in the hand specimen is methyl green (Ridgway). Some of the vesicles contain only celadonite, but others contain associated calcite and saponite.

---

[16] Ross, Clarence S., *op. cit.*, p. 3.

[17] Glocker, E. F., Generum et Specierum Mineralium secundum Ordines Naturales digestorum Synopsis, p. 193, *Halle* (**1847**).

[18] De Lish, Romé, Cristallographie, ou Description des formes propres à tous les corps du Regne mineral, **2,** 502, Paris (1783).

[19] *Hoffmann-Bergmannisches Jour.*, 519 (**1788**).

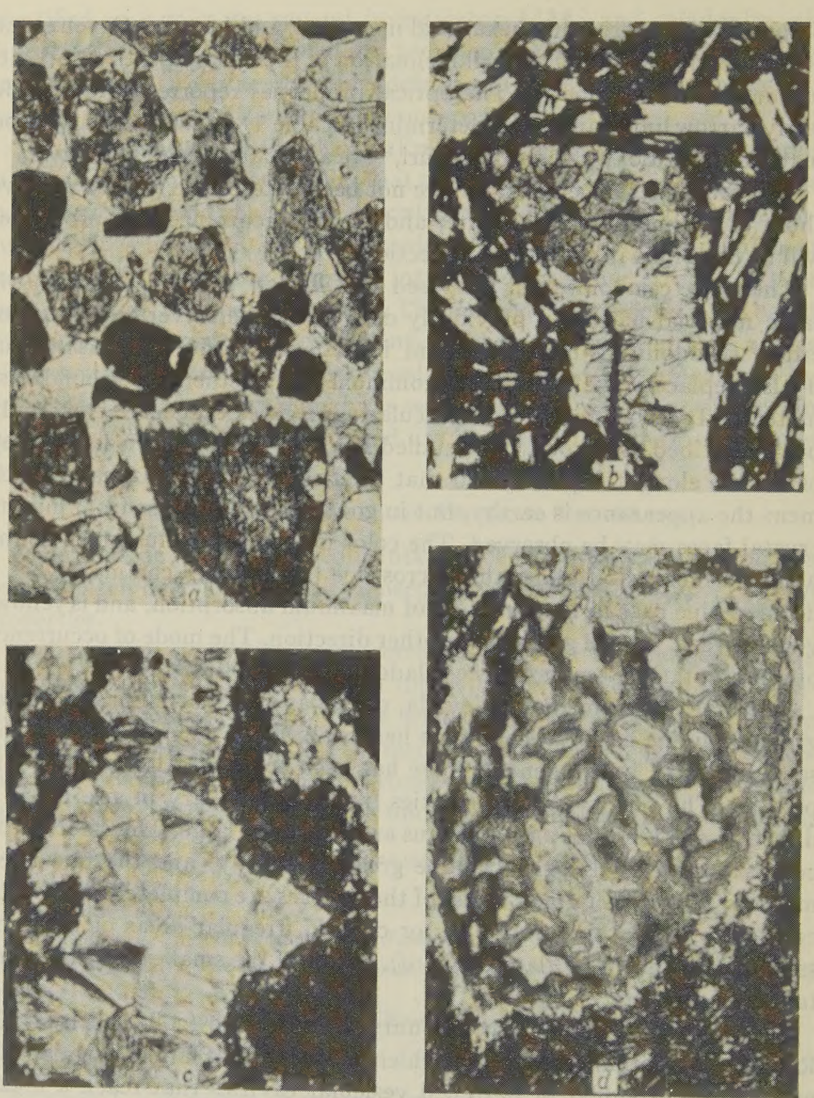

Plate 1

Glauconite and celadonite

Fig. (*a*). Altered volcanic materials, Center Point, Arkansas. Dark grains in upper two-thirds of figure are phonolite rock fragments almost completely altered to glauconite. Large grain in lower one-third is augite replaced by glauconite. Light gray interstitial material is calcite. ×54.

Fig. (*b*). Large central portion is a phenocryst of olivine in basalt; nearly fresh in lower portion, but upper part (gray) has been replaced by celadonite. White areas, plagioclase; black, groundmass. Locality unknown. ×54.

FIG. (*c*). Celadonite filling of cavity in basalt, Sandoval County, New Mexico. Radial, bladed habit is typical of celadonite. ×54.

FIG. (*d*). Celadonite filling vesicle in basalt, Reno, Nevada. Gray portion celadonite, nearly white areas are saponite. ×40.

Optical properties of these samples and of one from Kern County, California, are given in Table 1. The x-ray powder diffraction patterns of these samples of celadonite and of glauconite showed no observable differences.

TABLE 1. OPTICAL PROPERTIES OF CELADONITE AND GLAUCONITE

Locality	Indices of refraction			Birefringence $\gamma-\alpha$	Optical character and 2V	Pleochroism[a]	
	α	β	γ			X	Y and Z
Celadonite							
Reno, Nev.	1.610		1.641	.031	—	Pale yellow green	Guinea green
Sandoval Co., N. Mexico	1.606		1.634	.028	—	Dull yellow green	Skobeloff green
Red Rock Canyon, Kern Co., Calif.	1.606		1.635	.029	—	Light yellow green	Ethyl green
Glauconite†							
Bonne Terre, Mo.	1.597	1.618	1.619	.022[b]	−20°	Lemon yellow	Dark Russian-green

[a] Color names following Ridgway.

† Ross, Clarence S., *op. cit.*

[b] $r>v$ distinct.

METHOD OF CALCULATING FORMULAS FOR MINERALS HAVING SILICATE LAYER LATTICES

The significance of the kind and extent of isomorphous replacements in the micas was first recognized by Maugin.[20] Elucidation of the general structural scheme of mica is due to Pauling[21] who further showed that a large group of minerals have related structures. Among these are micas, brittle micas, chlorites, vermiculites, stilpnomelanes, hydrous micas, pyrophyllite, talc, montmorillonite, beidellite, nontronite, saponite, cronstedite, glauconite, celadonite, and the kaolin minerals.

---

[20] Maugin, C., Étude des micas au moyen des rayons X: *Compt. Rend.*, **186**, 879–881, 1131–1133 (1928).

[21] Pauling, L., The structure of the micas and related minerals: *Proc. Nat. Acad. Sci.*, **16**, 123–129 (1930).

The mica-like minerals have the common structural feature of tetrahedral groups of oxygen ions about silicon ions, joined into a hexagonal layer by sharing of oxygen ions by two tetrahedra. Two such layers are joined by octahedral coordination about Al''', Mg'', etc., of oxygen ions that are not shared between tetrahedra. The potassium ions fit between two such composite layers and have twelve neighboring oxygen ions.

The succession of atomic layers along the normal to the micaceous cleavage of muscovite and phlogopite and their idealized chemical formulas are:

	Muscovite		*Phlogopite*
Interlayer Nx	K^+	Nx	K^+
	$6O^{--}$		$6O^{--}$
Tetrahedral	$1Al^{+++}3Si^{++++}$	$1Al^{+++}3Si^{++++}$	
	$4O^{--}2(OH^-, F^-)$		$4O^{--}2(OH^-, F^-)$
Octahedral	$4Al^{+++}$		$6Mg^{++}$
	$4O^{--}2(OH^-, F^-)$		$4O^{--}2(OH^-, F^-$
Tetrahedral	$1Al^{+++}3Si^{++++}$		$1Al^{+++}3Si^{++++}$
	$6O^{--}$		$6O^{--}$
Interlayer	K^+		K^+

Muscovite $K \cdot (Al_2) \cdot (Al, Si_3) \cdot O_{10} \cdot (OH, F)_2$

Phlogopite $K \cdot (Mg_3) \cdot (Al, Si_3) \cdot O_{10}(OH, F)_2$

General knowledge of silicate structures[22] leads to the following expected types of isomorphous replacements in the micas:

Interlayer positions	K^+, Na^+, Rb^+, Cs^+, Ca^{++}, Ba^{++}, Sr^{++}
Tetrahedral positions	Si^{++++}, Al^{+++}
Octahedral positions	Al^{+++}, Ti^{++++}, Fe^{+++}, Fe^{++}, Mn^{++}, Cr^{+++}, Mg^{++}, Li^+

A remaining question to be answered for the micas is the actual extent to which various replacements take place.

In the montmorillonite-nontronite group of minerals, and in the hydrous micas, the interlayer positions are not completely filled, and the present study indicates that this is also true for glauconite and celadonite. The analyses of glauconite and celadonite show a potash ratio varying from 1, the value normal for micas, down to 0.56, with but 7 below 0.75; the average being 0.842. Thus the deviation from complete filling of the interlayer positions is significant, but not excessive. This must be taken into account in the formula which will be of the general type X_A(Al, Fe'''.

[22] Bragg, W. L., *Atomic Structure of Minerals*, Ithaca (**1937**).

Fe'', etc.$)_{\Sigma}(Al, Si)_4O_{10}(OH, F)_2$, where A is 1.00 or less and Σ is the number of octahedral positions filled, which must be 3.0 or less. The equivalence of the external base X is determined by the valence and number of the ions having octahedral coordination. A convenient method for calculating a formula is to reduce the analytical values of the ions having octahedral and tetrahedral coordination to their molal (M) values. It then is assumed that Al is distributed between tetrahedral and octahedral coordination so as to have $\Sigma = 2.00$. Thus $2(M(\text{Al}) + M(\text{Fe}''') + M(\text{Fe}'') + M(\text{Mg})$ etc. $-y) = (M(\text{Si}) + y)$ from which y, the molal amount of Al in tetrahedral coordination, can be evaluated. Amounts of the various ions in the formula then are obtained by multiplying their molal values by $4.00/(M(\text{Si}) + y)$. The subscript (A) of X, the interlayer cation, is then fixed by the amount of charge required to balance the lattice. In general it will not be equal to the equivalence of the interlayer ions. It is brought into agreement by change of Al between octahedral and tetrahedral coordination, Σ being finally greater or less than 2.00. In only 2 of the 42 analyses used in this study is the value of Σ below 2 and in most of them it is slightly, but significantly above 2.

Glauconite specimen number 14 is treated here as an example:

	%	Divide by	Mols			Equivalents		
SiO_2	49.4	60.06	Si	.822				
Al_2O_3	10.2	50.99	Al	.200	Sum .555			
Fe_2O_3	18.0	79.84	Fe'''	.225				
FeO	3.1	71.84	Fe''	.043				
MgO	3.5	40.32	Mg	.087				
CaO	0.6	28.04				Ca	.021	Sum .174
K_2O	5.1	47.10				K	.108	
Na_2O	1.4	31.00				Na	.045	

The next step is to calculate y from the condition $2[.555 - y] = [.822 + y]$, which gives y equal to .096. Thus $.822 + y = .916$, and the factor by which the molal quantities are to be multiplied to derive the trial formula is $4.00/.916 = 4.367$. This gives $.822 \times 4.367 = 3.59$ silicon atoms and a trial formula is $X_A[Al_{.46}Fe'''_{.98}Fe''_{.18}Mg_{.38}]\ [Si_{3.59}Al_{0.41}]\ O_{10}(OH)_2$. The sum of the cation valences indicated in the foregoing formula is 21.03, but the total cation valences must be 22 to balance the 10 oxygen ions, plus 2 hydroxyls. The difference of .97 must be supplied by Ca, K, and Na, and gives the value of X_A. However, the equivalence of Ca, K, and Na combined is only $.174 \times 4.367 = .76$. In order to bring these two quantities into agreement, aluminum must be transferred from tetrahedral to octahedral coordination. This is done by trial and error, always bearing in mind that as aluminum is transferred, the factor by which the molal amounts are to be multiplied changes. In this manner the formula is found to be:

$$X_{.75}[\mathrm{Al}_{.51}\mathrm{Fe}'''_{.99}\mathrm{Fe}''_{.18}\mathrm{Mg}_{.38}]\ [\mathrm{Si}_{3.63}\mathrm{Al}_{.37}]\mathrm{O}_{10}(\mathrm{OH})_2$$

EFFECT OF IMPURITIES

Submicroscopically crystalline micaceous minerals are very likely to contain fine-grained impurities. Appreciation of this factor, however, has led to an unnecessary assumption that impurities are so invariably present that no formula is justified.[23]

Glauconite being of sedimentary origin is commonly associated with coarse-grained detrital minerals, but that associated with clean crystalline limestones, or occurring in nearly pure beds, may be very free from accessory impurities. The glauconite can readily be concentrated by suspending it in water or by suitable heavy solutions, and only intergrown impurities need be feared. Possible fine-grained impurities are submicroscopically crystalline or amorphous phosphates and silica, leucoxene, calcium and iron carbonates, clay minerals, and oxides and hydrous oxides of iron. Small grains of phosphatic material (probably collophanite) are commonly associated with glauconite, and are only completely removed by careful hand picking. While many such impurities can now be recognized, much of the earlier work was carried out on more questionable material, and many of the modern glauconites associated with detrital materials are obviously quite impure. Clay minerals have a lower index of refraction and would be easily observable, and oxides and hydrous oxides of iron produce color changes warning of their presence. Sulfates, sulfides, chlorides, phosphates, or carbonates when present are adequate evidence of an impure sample.

Impurities that may be associated with celadonite are calcite, zeolites, saponite, serpentine, and cristobalite, common minerals in vesicular cavities of basalt, and oxides and hydrous oxides of iron resulting from subsequent oxidation. These impurities, with the exception of cristobalite and perhaps iron-rich saponite, are readily detected and probably were avoided in most samples selected for analysis. Cristobalite has to be accepted as a possible adventitious material in all samples which were not subjected to thorough microscopic examination.

Minor amounts of titanium and phosphorus have not been included in the calculations since it was thought that they were more likely to be present as impurities.

---

[23] Galliher, E. W., Glauconite genesis: *Bull. Geol. Soc. Am.*, **46**, No. 9, 1351–1365 (1935).

CHEMICAL RELATIONS OF GLAUCONITE AND CELADONITE

Analyses of forty-one glauconite samples all taken from the literature, are listed in Table 2. These include fifteen samples previously considered by Ross[24] and nine samples analyzed by Glinka.[25] The remainder of the analyses were obtained from the sources indicated in the footnotes to the table. Eight recent analyses, made since 1930, are included among these.

Glinka carried out gravity separations using Thoulet's solution. This would induce replacement of exchangeable base,—which is of the order of one-tenth of the interlayer base,—by potassium, but should not otherwise be confusing if the heavy solution was completely removed. An excess of potassium would not effect the other constituents, and these are the ones that are most significant in the following calculations. Some of Glinka's samples probably contained calcium carbonate as an impurity, this being particularly true for samples 38 and 39 of Table 2. The small amount of calcium in samples 4 and 5 was also regarded as an impurity. Samples 13 and 32 from other sources also probably contained calcium carbonate as an impurity.

---

[24] Ross, C. S., *loc. cit.*

[25] Glinka, K., *op. cit.*

TABLE 2. ANALYSES OF GLAUCONITE

	(1)	(2)	(3)	(4)	(5)	(6)	(7)	(8)	(9)	(10)	(11)	(12)	(13)
SiO_2	47.88	47.6	48.5	51.00	49.53	49.0	50.70	49.12	46.70	49.75	48.66	49.09	49.67
Al_2O_3	14.94	9.9	9.0	9.93	5.84	9.2	19.80	7.09	5.52	7.82	8.46	18.19	9.29
Fe_2O_3	17.13	21.9	20.0	18.69	20.06	19.5	—	25.95	21.62	22.26	18.80	6.42	19.88
FeO	2.68	1.5	3.1	1.98	5.95	3.3	8.60	0.89	2.42	2.36	3.98	2.56	1.28
MgO	2.45	3.7	3.7	3.85	2.92	3.6	3.70	3.10	4.16	3.25	3.56	3.10	4.03
CaO	0.56	0.8	0.4	0.87	0.56	0.5	—	—	0.63	—	0.62	1.03	1.95
K_2O	8.04	5.3	6.1	7.66	9.31	6.3	8.20	7.02	6.97	9.01	8.31	5.62	3.68
Na_2O	0.43	1.4	1.5	0.35	0.46	0.9	0.50	—	1.73	0.30	0.00	0.23	3.00
H_2O (ign)	5.91	7.7	7.3	5.83	4.91	7.6	8.50	7.12	11.48	5.16	6.56	13.47	7.88
Total	100.02	99.8	99.6	100.16	99.54	99.9	100.00	100.29	101.23	99.91	99.08[a]	99.90[b]	100.66

[a] Including $P_2O_5=0.12\%$; $MnO=0.01\%$.

[b] Including $TiO_2=0.21\%$.

TABLE 2. (*Continued*)

	(14)	(15)	(16)	(17)	(18)	(19)	(20)	(21)	(22)	(23)	(24)	(25)	(26)
SiO_2	49.4	49.09	48.12	51.95	49.42	51.00	49.23	50.36	51.24	51.35	52.96	49.76	50.58
Al_2O_3	10.2	15.21	9.16	17.81	10.23	9.93	7.11	7.04	12.22	9.47	12.76	8.18	6.72
Fe_2O_3	18.0	10.56	19.10	6.17	16.01	18.69	20.89	19.13	13.44	16.37	13.56	16.00	19.50
FeO	3.1	3.06	3.47	3.87	3.00	1.98	3.06	3.95	3.06	4.75	2.34	3.77	2.96
MgO	3.5	2.65	2.36	4.76	3.78	3.85	3.44	4.08	3.93	3.17	4.11	3.97	4.10
CaO	0.6	0.55	0.76	0.53	0.31	0.87	tr	0.91	0.10	0.63	—	0.41	0.34
K_2O	5.1	6.05	7.08	4.04	7.91	7.66	8.51	6.62	7.50	7.34	8.69	7.57	8.26
Na_2O	1.4	1.21	0.22	1.06	0.26	0.35	0.11	1.58	0.31	1.22	0.47	0.52	0.04
H_2O (ign)	8.3	11.64	10.06	9.43	8.08	5.83	6.71	6.32	8.20	4.85	4.91	9.82	7.76
Total	99.6	100.02	100.33	99.81[c]	99.80[d]	100.16	99.06	100.34[e]	100.00	99.50[f]	99.80	100.00	100.83[g]

[c] Including $P_2O_5=.02\%$; $TiO_2=.10\%$; $MnO=.07\%$.

[d] Including insoluble=0.80%.

[e] Including $TiO_2=.02\%$; $P_2O_5=.26\%$; $MnO=.06\%$; $Li_2O=.01\%$.

[f] Including $P_2O_5=0.35\%$.

[g] Including $P_2O_5=0.27\%$; $CO_2=0.30\%$.

TABLE 2. (*Continued*)

	(27)	(28)	(29)	(30)	(31)	(32)	(33)	(34)	(35)	(36)	(37)	(38)	(39)	(40)
SiO_2	51.15	49.47	51.11	52.74	51.55	49.81	55.95	51.90	54.58	50.62	46.90	42.32	41.02	47.59
Al_2O_3	7.61	5.59	4.88	12.29	4.03	6.33	11.56	1.52	7.17	3.80	4.06	16.51	22.19	17.99
Fe_2O_3	18.83	19.46	22.67	9.35	22.17	13.24	9.99	27.98	18.27	21.03	27.09	18.91	18.49	13.95
FeO	2.78	3.36	3.20	6.30	3.54	5.81	2.02	1.26	2.86	6.02	3.60	2.80	2.06	3.70
MgO	4.54	3.96	3.52	4.05	3.86	4.50	6.77	4.67	2.95	0.57[m]	0.70	1.74	0.69	1.80
CaO	—	0.60	0.52	0.55	0.69	1.58	3.95	0.89	1.86	0.54[m]	0.20	2.20	1.96	1.22
K_2O	7.80	8.04	6.88	7.97	7.03	7.45	4.12	4.90	5.34	7.14	6.16	7.49	5.74	7.21
Na_2O	—	0.16	0.63	0.09	0.55	0.16	0.61	0.53	1.23	—	1.28	0.42	0.38	0.42
P_2O_5	—	—	—	—	—	—	0.18	0.11	—	—	—	—	—	—
H_2O (ign)	7.56	8.54	6.34	5.93	6.62	9.70	4.82	6.15	6.53	9.14	9.25	7.48	7.88	5.27
Total	100.27	100.80[h]	99.75	99.40[i]	100.04	99.89[j]	99.97[k]	99.91[l]	99.48	99.86	99.24	99.87	100.41	99.15

[h] Including $P_2O_5=1.06\%$; $CO_2=0.56\%$.

[i] Including $F=0.13\%$.

[j] Including $P_2O_5=0.33\%$; $CO_2=0.98\%$.

[k] Including $TiO_2=0.59\%$.

[l] Including $TiO_2=0.30\%$.

[m] Including carbonates.

NOTE TO TABLE 2

C. O. Hutton and F. T. Seelye in an article on "Composition and properties of some New Zealand glauconites, *Am. Mineral.*, **26**, 595–604 (1941), give seven glauconite analyses. Their results calculated after the manner described in this paper lead to the following formulas:

Hutton and Seelye sample number	Tetrahedral coordination Si	Octahedral coordination				Interlayer cations X	No. of ions in octahedral coordination	Fe‴/Fe″
		Al	Fe‴	Fe″	Mg			
1	3.64	0.60	0.89	0.09	0.49	.73	2.07	9.9
2	3.89	0.39	1.00	0.22	0.38	.74	1.99	4.5
3	3.83	0.11	1.27	0.20	0.44	.75	2.02	6.3
4	3.46	0.13	1.49	0.19	0.35	.60	2.16	7.8
5	3.75	0.45	1.02	0.20	0.37	.71	2.04	5.1
6	3.55	0.18	1.29	0.41	0.25	.72	2.13	3.1
7	3.66	0.22	1.26	0.24	0.32	.78	2.04	5.2

The analyses apparently were made on very well selected materials and the results are in harmony with the general treatment of this paper.

TABLE 2—REFERENCES

1. Jurassic sandstone of Tschernofskoje. Glinka #5.
2. F(7) From unconsolidated Pleistocene west of San Pedro, California. Schneider, Hyrum, *Jour. Geol.*, **35**, 289–310 (1927).
3. F(5) From Franconia formation (Cambrian) near Norwalk, Wisconsin. Thomas B. Brighton, analyst. Schneider, Hyrum, *op. cit.*
4. Chalky sandstone of Padi. Glinka #1.
5. Eocene sandstone of Urals. Glinka #3.
6. F(4) From Hornerstown marl, Woodstown, New Jersey. Schneider, Hyrum, *op. cit.*
7. Island Orleans, Quebec. Hunt, T. S., *Geol. Canada* (**1863**), p. 487. Ross #4.
8. Pacific Ocean off Panama. Caspari, W. A., *Proc. Roy. Soc. Edinburgh*, **30**, 364–373 (1910). Ross #17.
9. F(8) From limestone near Palermo. Comucci, P., *Rend. Acc. Lincei Roma*, **30**, 220–224 (1921).
10. Chalky sandstone from Nasonovo. Glinka #2.
11. St. Joseph Lead Co. Mines. G. V. Brown, analyst. Ross #11.
12. Sandstone near Skole, Poland. Smulikowski, K., *Arch. Min. Soc. Sci. Varsovie*, **12**, 145–180 (1936); *Mineral. Abst.*, **6**, 345 (1936) (F).
13. F(1) From the Kupsten. Johnsen, A., *Scharf. Phys. Ökon Ges Königsberg*, **1**, 51–60 (1908).
14. F(6) From dolomite at the base of the Tempealeau (Upper Cambrian), northwest of Norwalk, Wisconsin. Schneider, Hyrum, *op. cit.*
15. Ashgrove, Elgin, Scotland. Heddle, M. F., *Trans. Roy. Soc. Edinburgh*, **29**, 79 (1879). Ross #15.
16. Lewes, Sussex. Radley, E. G., *Mineral. Mag.*, **19**, 331 (1920–22). Ross #12.
17. South Tyrol. Hummel, K., *Chemie der Erde*, **6**, 468–551 (1931).

18. Suir River, Olonets, Russia. Kupffer, A., *Archiv. Naturk, Liv.-, Ehst.- u. Kurlands, Ser I, Min. Wiss. Dorpat.*, **5**, 123 (1870). Ross #9.
19. Tertiary sandstone of Traktemiroff. Glinka #4.
20. Big Goose Canyon, near Sheridan Big Horn Mts., Wyoming. G. Steiger, analyst. *U. S. Geol. Survey, Bull.* **591**, 340 (1915). Ross #10.
21. Monte Brion, Lake Garda, Italy. *Sitzungsb. Akad. München*, **26**, 545 (1896). Ross #7.
22. Karga-Oro, Ontika, Esthonia. Kupffer, A., *Archiv. Naturk., Liv.-, Ehst.-, u. Kurlands, Ser I, Min. Wiss. Dorpat.*, **5**, 123 (1870). Ross #8.
23. F(2) From Silurian limestone, Eriksöre, Öland Sahlbom, Naima, *Geol. Inst. Univ. Upsala, Bull.* **15**, 211–212 (1916).
24. Lower Silurian limestone of Udriass. Glinka #10.
25. Grodno, Poland. Kupffer, A., *Archiv. Naturk., Liv.-, Ehst.-, u. Kurlands, Ser I, Min. Wiss. Dorpat.*, **5**, 123 (1870). Ross #2.
26. Sewell, N. J. Mansfield, G. R., *Econ. Geol.*, **15**, 557 (1920). Ross #5.
27. Agulhas Bank, South Africa. Caspari, W. A., *Proc. Roy. Soc. Edinburgh*, **30**, 364–373 (1910). Ross #6.
28. Elmwood Road, N. J. Mansfield, G. R., *Econ. Geol.*, **15**, 557 (1920). Ross #3.
29. Average analysis of seven samples from Tertiary. Takahashi, J. I., *Recent Marine Sediments*, 503–512 (1939).
30. F(3) From Schoen. Johnsen, A., *op. cit.*
31. Upper Cretaceous from Hokkaido. Takahashi, J. I., *Recent Marine Sediments*, 503–512 (1939).
32. F(9) From Marine Cretaceous, Zurawska region. Kampioni-Zakrzewska, *Ach. Min. Tow. Nauk Warsaw*, **13**, 9–17 (1937).
33. Monterey bay, California. A. A. Hanks, analyst. See number 34.
34. Galliher, E. W., *Bull. Geol. Soc. Am.*, **46**, 1359 (1935).
35. Recent sediment from Aomori Bay. Takahashi, J. I., *Recent Marine Sediments*, 503–512 (1939).
36. Havre, France. Haushofer, K., *Jour. Prakt. Chemie*, **102**, 38 (1886). Ross #1.
37. Agulhas Bank, South Africa. von Gumbel, C. W., *Sitzungsb. Akad. Wiss. München*, **16**, 417–449 (1886). Ross #16.
38. Jurassic sandstone of Karowo. Glinka #6.
39. Another fraction of 38. Glinka #7.
40. Jurassic sandstone of Kosolopowo. Glinka #9.

Formulas calculated from thirty-two of the glauconite analyses are listed in Table 3. Satisfactory formulas were not obtained for the remaining eight samples, which are listed in Table 2, chiefly to show the effect of impurities. Samples 33, 35, 38, 39, and 40 contained unduly large amounts of calcium, indicating a poor selection of material. Samples 33 and 35 further contained more SiO_2 than any of the other samples. Samples 33 and 34 are recent marine sediments that were known to be mixed with large amounts of other materials.[26] However, if sample 34 is predominantly glauconite, the low amount of Al_2O_3 that it contains would lead to formulas differing considerably from the ones obtained for the first thirty-two samples. Samples 36 and 37 are two samples previously discussed by Ross.[27] Formulas for them are:

---

[26] Galliher, E. W., Glauconite genesis: *Bull. Geol. Soc. Am.*, **46**, 1351–1366 (1935).

[27] Ross, C. S., *loc. cit.*

(36) $X_{.80}(Al_{.21}Fe'''_{1.26}Fe''_{.40}Mg_{.07})(Si_{3.85}Al_{.15})O_{10}(OH)_2$
(37) $X_{.85}(Al_{.03}Fe'''_{1.59}Fe''_{.24}Mg_{.08})(Si_{3.65}Al_{.35})O_{10}(OH)_2$

Their MgO contents are very much less than that of the remaining samples and the Al_2O_3 contents also are low. The value of Σ, the total number of ions having octahedral coordination, for each sample is 1.94. While this is not an impossible situation it is indicative of an unusual condition of formation and might be the result of later alteration.

Table 3. Glauconite Formulas

Sample number	Interlayer cations X	Octahedral coordination				Tetrahedral coordination Si	No. of ions in octahedral coordination	Fe'''/Fe''
		Al	Fe'''	Fe''	Mg			
1	.86	0.69	0.93	0.16	0.26	3.44	2.04	5.8
2	.81	0.36	1.21	0.09	0.40	3.50	2.06	13.4
3	.83	0.35	1.12	0.19	0.40	3.58	2.06	5.9
4	1.00	0.25	1.28	0.08	0.33	3.58	1.94	16.0
5	1.00	0.14	1.17	0.39	0.33	3.61	2.03	3.0
6	.79	0.40	1.08	0.20	0.40	3.61	2.08	5.4
7	.78	1.27	0.51		0.39	3.61	2.17	
8	.66	0.22	1.43	0.05	0.34	3.61	2.04	28.6
9	.98	0.12	1.26	0.15	0.48	3.62	2.01	8.4
10	.87	0.29	1.22	0.14	0.35	3.62	2.00	8.7
11	.86	0.36	1.06	0.24	0.39	3.62	2.05	4.5
12	.72	1.20	0.35	0.16	0.34	3.63	2.05	2.2
13	.87	0.42	1.08	0.08	0.42	3.63	2.00	13.5
14	.75	0.51	0.99	0.18	0.38	3.63	2.06	5.5
15	.83	0.94	0.58	0.19	0.29	3.63	2.00	3.0
16	.83	0.44	1.08	0.22	0.27	3.63	2.01	4.9
17	.56	1.12	0.33	0.22	0.50	3.65	2.17	1.5
18	.83	0.54	0.90	0.19	0.41	3.65	2.04	4.7
19	.88	0.52	1.01	0.12	0.31	3.67	1.96	8.4
20	.81	0.28	1.18	0.19	0.38	3.67	2.03	6.2
21	.98	0.28	1.05	0.24	0.44	3.67	2.01	4.5
22	.73	0.73	0.73	0.18	0.42	3.69	2.06	4.1
23	.93	0.50	0.88	0.28	0.39	3.69	2.05	3.1
24	.84	0.76	0.71	0.14	0.43	3.71	2.04	5.1
25	.87	0.44	0.91	0.24	0.44	3.72	2.03	3.8
26	.85	0.31	1.08	0.18	0.45	3.72	2.02	6.0
27	.74	0.37	1.03	0.17	0.50	3.72	2.07	6.0
28	.91	0.24	1.11	0.21	0.44	3.74	2.00	5.3
29	.83	0.17	1.25	0.20	0.38	3.75	2.00	6.2
30	.78	0.79	0.50	0.36	0.44	3.75	2.09	1.4
31	.85	0.35	1.22	0.21	0.42	3.78	2.10	5.8
32	.86	0.41	*0.77*	*0.37*	*0.52*	*3.84*	2.07	2.1

TABLE 4. ANALYSES OF CELADONITE

	(1)	(2)	(3)	(4)	(5)	(6)	(7)	(8)	(9)	(10)
SiO_2	55.61	53.23	50.6	54.30	54.73	52.69	55.30	50.70	57.72	56.41
Al_2O_3	0.79	2.13	4.2	5.08	7.56	5.79	10.90	4.72	0.33	2.14
Fe_2O_3	17.19	20.46	14.1	14.77	13.44	9.75	6.95	15.34	17.05	14.07
FeO	4.02	4.14	3.3	4.82	5.30	5.37	3.54	2.00	3.73	5.10
MgO	7.26	5.67	6.4	6.05	5.76	8.54	6.56	9.32	3.84	5.91
MnO	0.09	—	—	0.09	—	0.31	—	tr	0.08	0.23
CaO	0.21	—	3.1	0.80	0.00	1.16	0.47	1.32	0.60	0.60
K_2O	10.03	7.95	8.7	4.85	7.40	6.21	9.38	4.44	5.55	8.83
Na_2O	0.19	—	0.4	3.82	—	0.39	0.00	0.29	0.42	—
H_2O (ign)	4.88	6.18	8.3	5.64	6.40	10.48	6.51	12.52	10.78	6.80
Total	100.27	99.76	99.1	100.22	100.59	100.69	99.61	100.65	100.10	100.09

TABLE 4—REFERENCES

1. From vesicular basalt, 23 miles E. of Reno, Nevada. Wells, R. C., analyst. *U. S. Geol. Survey, Bull.* **878,** 102 (1937).
2. Bentonico, Monte Baldox, Italy. Levi, M. G., *Rivista di Min. e. Crist. Italiana,* **43,** 74 (1914).
3. From basalt, Sandoval Co., New Mexico. Wells, R. C., analyst. *U. S. Geol. Survey, Bull.* **878,** 102 (1937).
4. Madagascar. Raoult, M., analyst. Lacroix, M. A., *Soc. franc. Mineral. Bull.* **39,** 90–95 (1916).
5. Four miles E. of Vaile, Arizona. Koenig, G. A., *Jour. Phila. Acad. Nat. Sciences,* **15,** 424–425 (1912).
6. Amygdules in porphyritic basalt. Tayport Fife. Heddle, M. F., *Trans. Roy. Soc. Scot.,* **29,** 101–104 (1879).
7. From Vesuvius. Maegdefrau, E., and Hofmann, U., *Zeits. Krist.,* **A98,** 31–59 (1937).
8. Amygdaloidal basalt, Toselli pass Eriteria. Scherillo, A., *Periodico Min. Roma,* **9,** 253–264 (1938).
9. Cavities in basalt, Scuir Mohr Island of Rum. Heddle, M. F., *loc. cit.*
10. Druses in basalt S. of Grants Causway, Ireland. Heddle, M. F., *loc. cit.*

Analyses of ten celadonite samples, two of them new and the others taken from the literature, are listed in Table 4. Samples 9 and 10, which were studied by Heddle[28] probably contain a little silica as an impurity, and associated saponite was reported in No. 6. Calcium present in sample 4 was assumed to be present as the carbonate although it is a minor constituent. Sample 8 also contains an excess of magnesia.

[28] Heddle, M. F., The minerals of Scotland: Celadonite: *Trans. Royal Soc. Scotland,* **29,** 102–104 (1879).

TABLE 5. CELADONITE FORMULAS

Sample number	Interlayer cations X	Octahedral coordination				Tetrahedral coordination Si	No. of ions in octahedral coordination	Fe'''/Fe''
		Al	Fe'''	Fe''	Mg			
1	.98	0.07	0.93	0.24	0.77	4.00	2.01	3.9
2	.72	0.08	1.13	0.25	0.62	3.91	2.08	4.5
3	.90	0.28	0.82	0.21	0.73	3.90	2.04	3.9
4	.96	0.30	0.80	0.29	0.64	3.88	2.03	2.7
5	.68	0.50	0.72	0.30	0.61	3.88	2.13	2.4
6	.78	0.37	0.55	0.33	0.95	3.88	2.22	1.7
7	.91	0.78	0.36	0.21	0.69	3.87	2.04	1.7
8	.67	0.20	0.87	0.12	1.05	3.78	2.24	7.3
Specimens definitely containing silica as an impurity. Maximum and minimum formulas are given								
9	.80	0.03	1.17	0.28	0.52	4.00	2.00	4.2
	.83	0.00	1.79	0.29	0.53	3.97	2.01	
10	1.00	0.19	0.81	0.33	0.67	4.00	2.00	2.5
	1.00	0.06	0.91	0.36	0.76	3.85	2.09	

GENESIS OF GLAUCONITE

The characteristics of glauconite occurrences are admirably described in the comprehensive works of Cayeux,[29] Collet and Lee,[30,31] and Hadding.[32]

Hadding from his critical review of the literature and his extensive observations on the glauconites of Sweden concluded: "On summing up the inferences that can be drawn from the investigation . . . we can say that glauconite is always marine, always sublittoral, always a shallow sea formation, as a rule formed in agitated water, as a rule formed under decreased deposition of detritus, often formed during negative sedimentation, . . . never formed in highly oxygenous water."

Ichimura[33] concluded from his examination of the glauconitic rocks of Formosa that the glauconite in general was formed from mud grains and is associated with the usual detrital minerals. He states: "Moreover, the mode of occurrence of glauconite grains suggests that they were subjected to sorting in some agitated water."

---

[29] Cayeux, L., *op. cit.*

[30] Collet, L. W., and Lee, G. W., Recherches sur la Glauconi: *Proc. Roy. Soc. Edinburg,* **26**, 238–278 (1906).

[31] Collet, L. W., *Les Dêpots Marins,* 132–194, Paris (1908).

[32] Hadding, A., *op. cit.*

[33] Ichimura, T., *op. cit.*

Twenhofel[34] concludes his review of the literature on glauconite with the statement: "The existing state of knowledge with respect to the origin of glauconite supports the view that it is a product of diagenesis and that the glauconitic particles were originally pellets of mud containing finely divided and colloidal clay and iron oxides; that in some as yet unknown manner the aluminum of the clay was removed and its place taken by colloidal iron, and potash, and colloidal silica was absorbed from sea water or surrounding materials . . . An environment intermediate between strongly reducing and strongly oxidizing seems necessary . . . "

There is no essential disagreement with the observation that glauconite forms only in a marine environment with muds as the primary material for its formation. It often is associated with decaying organic matter and pyrite is not infrequently present. Cayeux[35] noted three general types of occurrences: (1) associated with organic matter such as foraminifera, (2) pellets, and (3) pigmentary. Cayeux believed that organic matter was absent from the pellets and took this as evidence against necessary presence of organic matter in the formation of glauconite. Buchanan[36] and Takahasi and Yagi,[37] however, noted various degrees of glauconitization of coprolites and it is the current opinion that some glauconite pellets were coprolites. Hadding presents evidence that the glauconite grains were initially colloidal material that had been transported; some being still colloidal when incorporated into the sedimentary beds, while others had undergone crystallization.

Galliher[38] recently has noted the associtaion of glauconite with partially altered biotite and has suggested that green sand deposits formed from biotite. Murray and Phillippi[39] had earlier suggested that glauconite was derived from micas and potassium feldspars. Derivation from biotite can at most have only local application, and is out of harmony with earlier observations. Several objections to such an origin in general may be pointed out.

Mineral associations in many green sands indicate that large supplies of micas and feldspars are not necessary for glauconite formation.[40] Some of the green sand beds of New Jersey are many feet in thickness and are composed of nearly pure glauconite. The accumulation of biotite in such thickness and freedom from impurities would be impossible. The almost complete absence of normal detrital materials and especially of muscovite, the dominant mica in all materials derived from crystalline rocks, and a material resistant to alteration under marine conditions, is especially significant.

---

[34] Twenhofel, W. H., *Treatise on Sedimentation*, Baltimore, 453–460 (**1932**).

[35] Cayeux, L., *op. cit.*

[36] Buchanan, J. Y., On the occurrence of sulphur in marine muds, and nodules and its bearing on their mode of formation: *Proc. Roy. Soc. Edinburgh*, **18,** 19–20 (1890).

[37] Takahasi, J., and Yagi, T., The peculiar mud-grains in the recent littoral and estuarine deposits, with special reference of the origin of glauconite: *Econ. Geol.*, **24,** 838–852 (1929).

[38] Galliher, E. W., *loc. cit.*

[39] Murray, J., and Phillippi, E., *Die Grundprolien der deutschen Tiefsee-Exped. auf dem Dampfer "Valdiva," 1898-1899*, **10,** 177 (1908).

Glauconite has formed in association with biotite in arkosic Ordovician bentonites in Tennessee; that is, a bentonite whose characteristic mineral is a hydrous mica. The biotite which is nearly fresh in most Ordovician bentonite is bleached in this occurrence. It has acted as a locus for the deposition of glauconite so that the two minerals are in parallel orientation, but there has been no replacement of biotite by glauconite.

A recent study of rocks from the Panama Canal Zone composed of andesitic rock debris, has shown the presence of normal glauconite in rounded grains, together with another type that has formed by direct replacement of andesite rock grains and of augite.

Ross, Miser, and Stephenson[41] mention glauconite in association with volcanic materials from southwestern Arkansas. This material has formed under marine conditions and so its genesis is that of marine glauconite. This material has most commonly formed as a replacement of grains of phonolitic rock as shown by the mottled grains in the upper part of Plate 1, Fig. *a*; the gray portion being glauconite. Less commonly, glauconite has replaced augite as in the large grain at the bottom of the figure. The light gray interstitial material is calcite. In a few specimens glauconite has filled spaces between mineral and rock grains, where it has a structure indicating crystallization from material originally deposited as a colloid. In none of these occurrences is there any paragenetic relation to biotite. The origin of glauconite has also been discussed by Hadding.[42]

Attention is now directed to the glauconite formulas of Table 3, which were derived from analyses of specimens from many different deposits. They nevertheless show some remarkable regularities indicative of the common mode of origin for sedimentary glauconites. The magnesium content, referred to the general formula, is between 0.35 and 0.45 ion for twenty of the thirty-two analyses, and the maximum variation is from 0.26 to 0.52 ion. Silicon in tetrahedral coordination varies from 3.44 to 3.84 ions in the thirty-two samples, and all except four samples have between 3.58 and 3.75 ions. The interlayer ion content is definitely less than one equivalent, the mean value being 0.84. An average formula is:

---

[40] Note also, Correns, C. W., *Die Sedimentgesteine*, p. 209, Berlin (**1937**).

[41] Ross, Clarence S., Miser, Hugh D., and Stephenson, Lloyd D., Waterlaid volcanic rocks of early Upper Cretaceous age in southwestern Arkansas, southeastern Oklahoma, and northwestern Texas: *U. S. Geol. Surv., Prof. Paper* **154,** 184 (1928).

[42] Hadding, A., *op. cit.*

$$(K,Ca_{1/2},Na)_{.84}(Al_{.47}Fe'''_{.97}Fe''_{.19}Mg_{.40})(Si_{3.65}Al_{.35})O_{10}(OH)_2$$

Muds in general and all the finely divided detrital minerals, with the exception of hydrous micas, contain less magnesium than required by the above formula. An average formula derived from six hydrous mica analyses listed by Grim, Bray, and Bradley[43] is:

$$K_{.58}(Al_{1.38}Fe'''_{.37}Fe''_{.04}Mg_{.34})(Si_{3.41}Al_{.59})O_{10}(OH)_2$$

The hydrous micas vary in composition, the limits of which are undetermined, but the foregoing formula is probably representative enough to show the similarities and striking differences from glauconite.

The improbability of derivation from a material carrying adequate potassium, and the invariable formation under a marine environment, indicates that potassium was derived from the sea, and the same is, no doubt, true of magnesium. In this connection it may be pointed out that a bentonite from Mine Creek, Howard County, Arkansas, with several per cent of MgO, has formed from volcanic ash that contained but a fraction of a per cent of MgO; and since alteration occurred in a marine embayment, sea water was no doubt the source of the excess magnesium.[44]

The near constancy in the magnesia content of glauconites to 0.32 reflects the essentially unchanging nature of the environment and the structural requirements of the mineral lattice. The other constituents of glauconite, silicon, aluminum, and iron could adequately be supplied by any mud. There is thus no particular restriction on the type and composition of the source material.

The amount of aluminum having octahedral coordintaion in glauconite varies from 0.12 to 1.27 ions, with accompanying variations in the total amount of iron. It clearly is not constant and probably is not determinative in the formation of the mineral. Ferrous iron is characteristic of glauconite, and the value of Fe'''/Fe'' for half the samples is between 4.1 and 6.2. These are narrow limits considering the factors involved and the possibility of subsequent oxidation. However, it probably is not due to a particular reducing condition but rather to several different factors. Among these would be the requirements of the structure; and the possible precipitation of iron sulfide, which limits the concentration that ferrous iron could reach in the system in which glauconite is forming.

---

[43] Grim, R. E., Bray, R. H., and Bradley, W. F., Mica in argillaceous sediments: *Am. Mineral.*, **22,** 813–829 (1937).

[44] Ross, Clarence S., Miser, Hugh D., and Stephenson, Lloyd D., *op. cit.*, p. 187.

Factors influencing the availability of ferrous iron in a marine environment have been thoroughly considered by Cooper.[45] He shows that the potential in a system in which the equilibrium $Fe^{+++} + e^{-} \rightleftarrows Fe^{++}$ is established is given by $-E = [1.011 - 0.058 \log A_{Fe^{++}} - 0.174\ pH]$ volts, where $A_{Fe^{++}}$ is the activity of the ferrous iron and *pH* is the usual negative log of the hydrogen ion concentration. The system is assumed to be saturated with respect to the ferric ion. If the potential is -0.4 volt (which is strongly reducing) and the *pH* is 6.0 (which is as acid as the marine environment reasonably could be) the ferrous ion activity would be 4×10^{-8} gm. mols. per liter, which is very dilute. The oxidation reduction potential for the reaction $SO_4^{--} + 4H_2O \rightleftarrows S^{--} + 4H_2O(l)$ calculated from the standard free energies of SO_4^{--}, S^{--}, and $H_2O(l)$ is -0.14 volt. This is a much stronger reducing system than the ferric, ferrous system and will be adequate at any reasonable hydrogen ion concentration to reduce the iron.

The not uncommon occurrence of ferrous sulfide minerals with glauconite indicates that sulfate reducing bacteria might often create the necessary oxidation reduction potential for glauconite formation. Bacteria commonly are found in muds[46] and could use organic materials of plant and animal remains and coprolite pellets as food. However, this is equally true of other bacteria that reduce ferric compounds to ferrous ones.[47] The only essential factor is strongly reducing conditions, including almost complete absence of oxygen, and this necessarily requires the action of bacteria on organic matter.

The important point of these considerations is that ferrous iron necessary for glauconite formation appeared only as a result of bacterial action in a system of negligible oxygen content, that is, anaerobic. The ferrous iron concentration in solution was very small and the ferrous iron was fixed in some insoluble form having much lower solubility than the hydroxide, possibly in glauconite itself. However, it is probable that before or during the complete formation of glauconite the portion of the system containing ferrous iron was sometimes transported as a colloid.

The number of ions having octahedral coordination, Σ, varies between 2.00 and 2.09 for all except five of the samples. Glauconite thus is a heptaphyllite type of mica showing very limited solid solution toward an octaphyllite (biotite) type, despite the presence of Mg'' and Fe'' to the extent of $\frac{1}{4}\Sigma$ to $\frac{1}{3}\Sigma$. The average amount of aluminum in tetrahedral coordination is 0.35 ion which is greatly less than the amount, near 1.00 ion, found in the usual micas. The number of interlayer cations, K', Ca'', Na', is determined by these interrelations and while the maximum possible value is 1.00, it is not surprising to find actual amounts slightly less.

---

[45] Cooper, L. H. N., Some conditions governing the solubility of iron: *Proc. Roy. Soc.* (London), B, **124,** 299–307 (1938).

[46] Bastin, E. S. (Collaboration of Anderson, B., Greer, F. E., Merritt, C. A., and Moulton, G.), The problem of the natural reduction of sulfates: *Bull. Am. Soc. Petroleum Geologists* **10,** 1270–1299 (1926).

[47] Buchanan, R. E., and Fulmer, E. I., *Physiology and biochemistry of bacteria,* Baltimore, **3,** 211–216 (1930).

If glauconite is formed in the presence of normal ocean waters, then the ratios of the amounts of the interlayer ions are determined by competition, depending upon their affinity for the available sites in the crystal lattice and their concentration in the medium. The average interlayer ionic ratios in equivalents for glauconite are near

$$Na:Ca:K::0.15:0.20:1.0$$

A few samples deviate considerably from these ratios, which is not unexpected since glauconite did not necessarily form in normal ocean water or might have undergone later exchange of alkalis, although as previously pointed out there is a strong indication of a nearly uniform genetic environment for most of the samples. Ionic ratios in equivalents in ocean water are[48] Na:Ca:K::46.3:2.1:1.0. These combined into an affinity series give about Na:Ca:K::300:10:1. In other words for glauconite to contain equal amounts of Na' and K' the solution in contact would have to contain 300 times as much Na' as K'. The chemistry of the system from which micas form is not experimentally reproducible, and so glauconite formation under marine conditions where the chemistry of the system is approximately known is significant because it serves to illustrate the dominant formation of potash micas even from systems that were obviously rich in sodium.

Genesis of Celadonite

Formulas derived from analyses of celadonite are listed in Table 5. Samples 9 and 10 contained excess silica and for this reason maximum and minimum amounts of silicon in tetrahedral coordination were assumed. The maximum amount of course is 4.00 ions for the usual formula, and the minimum is that amount consistent with the amounts of the remaining constituents. These limits serve to emphasize the maximum possible effect of impurities.

There are three prominent features of these celadonite formulas. The magnesium content again is surprisingly constant, the average value per formula being 0.76 ion with three-fourths of the analyses in the range

---

[48] Clarke, F. W., The Data of Geochemistry: *U. S. Geological Survey, Bull.* 770, 127 (1924).

0.61–0.77 ion. In none of the samples is the Mg″ content as low as the highest value found for glauconite. Silicon in tetrahedral coordination is very high, the minimum value again being greater than the maximum value for glauconite. The total iron content varies greatly but a large fraction of it is ferrous which leads to a smaller value for Fe‴/Fe″ than generally found for glauconite. An average formula is:

$$(K,Ca_{1/2},Na)_{.82}(Al_{.34}Fe'''_{.76}Fe''_{.24}Mg_{.76})(Si_{3.89}Al_{.11})O_{10}(OH)_2$$

Celadonite is essentially a heptaphyllite mica, Σ, the number of ions in octahedral coordination, varying from 2.01 to 2.24, but it could not safely be held that Σ is truly greater than 2.13. Despite the heptaphyllite character about half the ions having octahedral coordination are doubly charged, Mg″ and Fe″. The lack of intralayer charge requiring presence of interlayer ions is almost entirely confined to positions with octahedral coordination. Samples number 1, the excellent specimen from the vicinity of Reno, Nevada, and number 9 are of particular interest in that they indicate that aluminum is not a necessary constituent of celadonite. Limiting formulas for samples number 1 and 9 could be:

$$(1)\ K_{1.0}(Fe'''_{1.00}Fe''_{.25}Mg_{.75})Si_{4.0}O_{10}(OH)_2$$
$$(9)\ K_{0.8}(Fe'''_{1.20}Fe''_{.30}Mg_{.50})Si_{4.0}O_{10}(OH)_2$$

Even though sample number 7 contains more aluminum than seven-tenths of the glauconite samples, it has less in tetrahedral coordination than any of them. This apparently is due to the higher magnesium content of celadonite which further emphasizes the determinative role of magnesium in the formation of glauconite.

A study of the rocks in which celadonite occurs gives significant information about the chemical relations which control its formation. The parent rock is usually a vesicular basalt, commonly an olivine basalt. Celadonite not only fills vesicular cavities in basalt but directly replaces olivine in a number of specimens. This is shown in Plate 1, Fig. *b*, where a phenocryst of olivine has been partly replaced by celadonite (gray material in upper portion), while the lower part represents only partly altered olivine. Olivine, $(Mg,Fe)_2SiO_4$, is an unstable mineral in the presence of water vapor and commonly is altered in the late cooling (deuteric) stages of a basalt. In most of the basalt specimens examined that contained celadonite, olivine has in general been largely altered to serpentine, a hydrous silicate of magnesium which often contains ferrous iron. On the other hand, iddingsite, another widely occurring deuteric alteration product of olivine, but one characterized by ferric iron,[49] is not

[49] Ross, Clarence S., and Shannon, Earl V., The origin, occurrence, composition, and physical properties of the mineral iddingsite: No. 2579, From the *Proc. U. S. Nat. Museum*, **67,** 1–19 (1925).

associated with celadonite, apparently because of the oxidizing conditions during its formation.

Celadonite, as well as glauconite, in many specimens has the appearance of having passed through a gel state in its formation, that is, it is now a metacolloid. Olivine in altering to celadonite could supply silicon, magnesium, and ferrous iron. However, some magnesium would have to be removed. Part of the ferrous iron would have to be changed to ferric iron, but the remaining ferrous iron would require that the environment be a reducing one. It would be necessary for all the potassium, as well as the aluminum, to be introduced from nearby material. On the other hand, material forming celadonite in vesicular cavities would all have to be transported, at least for short distances.

END MEMBER FORMULAS FOR GLAUCONITE AND CELADONITE

It is desirable when possible to give end formulas for minerals of variable composition. Derivation of a reasonable number of suitable end formulas for glauconite and celadonite, however, is a simplification since the composition of each is influenced by at least six variables. These variables are Al, Fe''', Fe'', and Mg having octahedral coordination, the number of ions between layers, and the amount of Al having tetrahedral coordination. A rigorous representation of the composition takes account of the fact that glauconite and celadonite are not strictly heptaphyllitic (the ions in octahedral positions normally exceed 2) and the interlayer bases (essentially K) are in general less than 1. These two factors are neglected in the end members represented in the following list. However, the representation of the composition by such end members is sufficiently close to illustrate the relationships of glauconite and celadonite within the mica group.

The most unusual features of glauconite and celadonite as essentially heptaphyllite micas is their considerable content of ferric iron and the predominance of silicon in tetrahedral coordination. Compositions of these minerals can approximately be represented by combination of the following six formulas, listed in the order of their abundance:

(1) $K(Fe'''Mg)Si_4O_{10}(OH)_2$
(2) $K(Fe'''Fe'')Si_4O_{10}(OH)_2$
(3) $K(AlMg)Si_4O_{10}(OH)_2$
(4) $K(AlFe'')Si_4O_{10}(OH)_2$
(5) $K(Fe''')_2AlSi_3O_{10}(OH)_2$
(6) $K(Al)_2AlSi_3O_{10}(OH)_2$

From these six formulas all possible combinations of Al, Mg, Fe''', and Fe'' in strictly heptaphyllite micas can be obtained.

Formula number (6) is that usually given for muscovite and number

(5) represents a ferric analogue of muscovite.[50] Analyses of sericites seem to trend towards the composition represented by formula (3). This formula and the remaining three formulas (1), (2), and (4) are characteristic of celadonite. Thus celadonite, sample number (1), can be represented by .77(1)+.16(2)+.07(4), and sample number (5), approximately by .58(1)+.20(4)+.12(6)+.10(2). Table 6 shows the close agreement between the chemical analyses and the compositions (in weight percentage) calculated on the basis of the foregoing interpretation; celadonites 1 and 5 being arbitrarily selected as examples:

TABLE 6. INTERPRETATION OF COMPOSITION OF CELADONITES 1 AND 5

Percentage	Celadonite 1	Percentage	Celadonite 5
77	$KFe'''MgSi_4O_{10}(OH)_2$	58	$KFe'''MgSi_4O_{10}(OH)_2$
16	$KFe'''Fe''Si_4O_{10}(OH)_2$	10	$KFe'''Fe''Si_4O_{10}(OH)_2$
7	$KAlFe''Si_4O_{10}(OH)_2$	19	$KAlFe''Si_4O_{10}(OH)_2$
—		13	$KAl_2AlSi_3O_{10}(OH)_2$
100	Total	—	
		100	Total

	Celadonite 1 Analysis	Celadonite 1 Calculated	Celadonite 5 Analysis	Celadonite 5 Calculated
SiO_2	55.61	55.82	54.73	54.55
Al_2O_3	0.79	0.83	7.56	7.25
Fe_2O_3	17.19	17.24	13.44	12.63
FeO	4.02	3.69	5.30	4.76
MnO	0.09		—	—
MgO	7.26	7.30	5.76	5.50
CaO	0.21		0.00	—
K_2O	10.03	10.94	7.40	11.08
Na_2O	0.19		—	—
H_2O	4.88	4.18	6.40	4.23
	100.27	100.00	100.59	100.00

That the celadonite type of formula, namely: $K(Fe''', Al)(Mg, Fe'')Si_4O_{10}(OH)_2$ greatly predominates in all the celadonites, is shown in Table 7. Analyses 6 and 8 must have been made on impure material, as a magnesium silicate (serpentine or saponite?) must have been present to account for the high percentages of MgO. These two analyses hence are omitted.

The last two columns show the great preponderance of the celadonite type of formula over that of the muscovite type, in all celadonites.

---

[50] Clarke, F. W., and Darton, N. H., On a hydromica from New Jersey: *U. S. Geol. Surv., Bull.* **167**, 155 (1880).

TABLE 7. INTERPRETATION OF ANALYSES OF CELADONITE

No.	Celadonite $K(Fe''', Al)(Mg, Fe'')Si_4O_{10}(OH)_2$ type				Muscovite $K(Fe''',Al)_2AlSi_3O_{10}(OH)_2$ type		Celadonite type	Muscovite type
	$Fe'''Mg$	$Fe'''Fe''$	AlMg	$AlFe''$	Fe'''	Al		
1	77	16	—	7	—	—	100	0
2	60	26	—	—	13	1	86	14
3	70	9	—	13	—	8	92	8
4	62	16	—	13	—	9	91	9
5	58	10	—	20	—	12	88	12
7	37	—	30	21	—	12	88	12
9	56	31	—	—	13	—	87	13
10	66	15	—	19	—	—	100	0

In the interpretation of the composition of the glauconites on this basis, more than one distribution of Al and Fe''' as between formulas 5 and 6 is possible. Glauconite 1 is arbitrarily taken as an example. All of the alumina may be considered as belonging to the muscovite type of formula, $K(Fe''', Al)_2AlSi_3O_{10}(OH)_2$, as given in Table 8, column 1, when the remaining constituents belong to the celadonite type of formula, $KFe'''(Mg, Fe'')Si_4O_{10}(OH)_2$ free from alumina. In the second interpretation the alumina is divided between the two types of formulas, as shown in column 3.

TABLE 8. INTERPRETATION OF GLAUCONITE 1

Percentage	1 Calculated	2	Percentage	3 Calculated
26	$KFe'''MgSi_4O_{10}(OH)_2$	Analysis	24	$KAlMgSi_4O_{10}(OH)_2$
17	$KFe'''Fe''Si_4O_{10}(OH)_2$		16	$KAlFe''Si_4O_{10}(OH)_2$
27	$KFe'''_2AlSi_3O_{10}(OH)_2$		49	$KFe'''_2AlSi_3O_{10}(OH)_2$
30	$KAl_2AlSi_3O_{10}(OH)_2$		11	$KAl_2AlSi_3O_{10}(OH)_2$
100	Total		100	Total
SiO_2	47.87	47.88		47.86
Al_2O_3	14.54	14.94		14.69
Fe_2O_3	17.30	17.13		17.15
FeO	2.67	2.68		2.69
MgO	2.47	2.45		2.44
CaO	—	0.56		—
K_2O	10.96	8.04		10.97
Na_2O	—	0.43		—
H_2O	4.19	5.91		4.20
	100.00	100.02		100.00

In either interpretation the muscovite type of formula which played only a minor role in the composition of the celadonites, now becomes of equal importance with the celadonite type of formula and in the interpretation shown in column 3, the ferric iron analogue of muscovite is the dominant component.

An arbitrarily selected group of glauconites, so chosen as to include a wide range in composition, may be approximately interpreted as having the following component composition:

TABLE 9. INTERPRETATION OF SELECTED ANALYSES OF GLAUCONITE

No.	Celadonite $K(Fe''', Al)(Mg, Fe'')Si_4O_{10}(OH)_2$ type				Muscovite $K(Fe''', Al)_2AlSi_3O_{10}(OH)_2$ type		Celadonite type	Muscovite type
	Fe'''Mg	Fe'''Fe''	AlMg	AlFe''	Fe'''	Al		
1	26	17	—	—	27	30	43	57
5	31	38	—	—	22	9	69	31
8	37	—	—	7	56	—	44	56
10	36	15	—	—	39	10	51	49
12	36	—	—	17	—	47	53	47
21	44	—	—	24	30	2	68	32
31	41	23	—	—	36	—	64	36

The marked increase of importance of the muscovite type of formula in the glauconites is shown in the last two columns.

This study has confirmed the close relationship of glauconite and celadonite and raises the question of retention of both names. While the composition of neither of these members of the mica group can be expressed by one formula, the essentially aluminum-free celadonites are dominantly $KFe'''(Mg, Fe'')Si_4O_{10}(OH)_2$ with Mg greatly in excess over Fe''. Glauconites, on the other hand, do not approximate any single simple formula but represent a much more extended series whose characteristics seem to be an approximate composition of about equal parts of the celadonite type formula, as given above, and the muscovite type of formula, with the ferric analogue of muscovite predominating.

As the well established term "glauconite" is used for a mineral of characteristic sedimentary origin whereas the term "celadonite" is used for a mineral of quite different occurrence and paragenesis, it seems best to retain both names.

ACKNOWLEDGMENTS

Dr. M. L. Fleischer of the United States Geological Survey greatly facilitated this work by his hearty cooperation; and Dr. W. T. Schaller has assisted in the calculations and contributed many helpful suggestions.

CONTRIBUTIONS TO THE MINERALOGY OF STERLING HILL, NEW JERSEY: MORPHOLOGY OF GRAPHITE, ARSENOPYRITE, PYRITE, AND ARSENIC

Charles Palache,
*Harvard University, Cambridge, Massachusetts.**

Graphite

No satisfactory data for the morphological determination of the symmetry and elements of graphite have hitherto been published. Goldschmidt (1918), unable to decide between Kenngott's hexagonal interpretation of his meager data and the monoclinic interpretation of Nordenskjöld, gives both in the *Atlas*. The former has, however, been accepted by most authors and the mineral has been described as hexagonal-rhombohedral, the triangular striations commonly to be seen on the base determining its rhombohedral classification. Recent studies of the structure cell by x-ray methods lead to the conclusion that graphite is hexagonal (Bragg, 1937) and not rhombohedral, although a trigonal symmetry class is not excluded.

The measurements presented in the following pages, made on graphite crystals from Sterling Hill, New Jersey, seem to the writer to yield a definite and unambiguous solution of this problem. Graphite is hexagonal with full symmetry.

The graphite crystals from Sterling Hill occur in crystalline limestone in an association to be described on a later page. I am indebted for them to Mr. L. H. Bauer of Franklin, New Jersey, who found the material and isolated the best crystals. They are scales up to 1 or 2 mm. in diameter, the best ones, however, not exceeding 0.5 mm. The base is extremely brilliant, hexagonal in outline, with edges showing many facets, often very plane and bright, although striated edges are the rule. Of the hundreds of crystals studied, ten were completely measured and yielded the forms and angles shown in Table 1. Four of these crystals were very simple in form and gave closely agreeing measurements for three forms only besides the basal pinacoid, which are regarded as definitely proving the hexagonal symmetry of graphite. They are summarized in Table 2.

But one of these crystals showed measurable faces at the lower end, and it was unfortunately lost in attempting to reverse it on the goniometer. Figures 1, 2 and 3 represent respectively crystals 1, 3 and 4 of Table 2 in approximately their actual development.

---

* Contribution from the Department of Mineralogy and Petrography, Harvard University, No. 248.

Table 1. Graphite: Measured Angles, 10 Crystals

Forms		Measured		Range		Calculated	Number of	
		ϕ	ρ	ϕ	ρ	ρ	faces	crystals
m	$10\bar{1}0$	30°14′	90°00′	0°00′–1°22′	—	90°00′	10	7
d	$10\bar{1}8$	30 53	20 49½	0 16 –1 29	20°49′–20°50′	21 10	2	1
e	$10\bar{1}5$	30 31	32 03	0 00 –1 32	30 38 –33 14	32 26½	4	3
t	$10\bar{1}4$	30 12	38 24	0 10 –0 14	37 48 –39 00	38 28	2	2
r	$10\bar{1}3$	30 29	46 59	0 02 –0 40	45 49 –48 30	46 39	8	4
o	$10\bar{1}2$	30 13	57 48	0 04 –0 22	57 10 –58 30	57 49	12	6
w	$20\bar{2}3$	30 26	64 43	0 04 –1 24	63 40 –65 45	64 44	4	3
x	$40\bar{4}5$	30 16	69 07	0 00 –0 40	68 23 –69 46	68 31½	4	3
p	$10\bar{1}1$	30 00	72 32	0 00 –0 05	72 21 –72 50	72 32	18	4
y	$20\bar{2}1$	30 20	81 10	0 15 –0 25	80 20 –82 00	81 03½	2	2
π	$11\bar{2}6$	0 38	42 35	0 07 –1 10	42 15 –42 55	42 32	2	1
ρ	$11\bar{2}3$	0 59	61 28	0 07 –2 09	59 00 –64 30	61 24½	7	4
ϕ	$11\bar{2}2$	0 09	70 02	0 03 –1 33	69 15 –70 40	70 02	6	1
σ	$22\bar{4}3$	1 05	74 40	0 00 –3 16	73 47 –75 40	74 45½	4	4
τ	$11\bar{2}1$	0 30	79 52	—	—	79 52	1	1

Table 2. Measurements of 4 Crystals of Graphite

		ϕ	ρ
Crystal 1			
p $10\bar{1}1$	6 faces	29°57½′± 2½′	72°27′ ± 5′
Crystal 2			
p $10\bar{1}1$	5 faces	29 51 ±14	72 37 ± 9
o $10\bar{1}2$	3 faces	29 50 ±12	57 18 ±18
Crystal 3			
p $10\bar{1}1$	4 faces	29 50 ±13	72 39 ±21
o $10\bar{1}2$	6 faces	29 50 ±13	57 42½±12
Crystal 4			
p $10\bar{1}1$	6 faces	29 55 ± 7	72 32 ±20
ϕ $11\bar{2}2$	6 faces	0 40 ±51	70 02 ±38

The other measured crystals were more complex. Figure 4 illustrates one of them and it is evident that individual forms are irregularly developed, no one pyramid having all its six faces present. But the distribution in this and in every crystal is not systematically trigonal but random. It is also true that other reflections were obtained from some crystals which were not in the dominant zones and which could not be simply indexed in the projection. But these were always subordinate to the prevailing hexagonal distribution.

From the mean values for the position angles shown in Table 1 the elements were calculated, using 69 faces of 11 forms on 10 crystals. The resulting value, $p_0=3.1780$, $c=2.7522$, is taken for the calculation of the angle table, Table 3.

TABLE 3. GRAPHITE: ANGLE TABLE

Hexagonal, Dihexagonal-dipyramidal 6/*m* 2/*m* 2/*m*
$a:c=1:2.7522$; $p_0:r_0=3.1780:1$

Forms	ϕ	ρ	M	A_2
c 0001	—	0°00′	90°00′	90°00′
m $10\bar{1}0$	30°00′	90 00	60 00	90 00
d $10\bar{1}8$	30 00	21 10	79 36	90 00
e $10\bar{1}5$	30 00	32 26½	74 26½	90 00
t $10\bar{1}4$	30 00	38 28	71 54	90 00
r $10\bar{1}3$	30 00	46 39	68 41	90 00
o $10\bar{1}2$	30 00	57 49	64 58	90 00
w $20\bar{2}3$	30 00	64 44	63 07	90 00
x $40\bar{4}5$	30 00	68 31½	62 16	90 00
p $10\bar{1}1$	30 00	73 32	61 31	90 00
y $20\bar{2}1$	30 00	81 03½	60 24	90 00
π $11\bar{2}6$	0 00	42 32	90 00	70 14½
ρ $11\bar{2}3$	0 00	61 24½	90 00	63 37½
ϕ $11\bar{2}2$	0 00	70 02	90 00	61 58
σ $22\bar{4}3$	0 00	74 45½	90 00	61 09½
τ $11\bar{2}1$	0 00	79 42	90 00	60 32

The elements calculated from *x*-ray measurements are $p_0=3.170$, $c=2.745$. The commonly accepted elements of graphite based on Kenngott's (1854) original measurements are, if *c* be doubled, $p_0=3.2006$, $c=2.7718$, but regarding this value see the remarks on a later page.

Confirmation of the results obtained from these measurements was found on a single crystal of graphite from Ticonderoga, New York, shown in Fig. 5. Although of much poorer quality than the Sterling Hill crystals, it gave mean angles for two forms which are comparable:

		ϕ	ρ
p $10\bar{1}1$	6 faces	29°57′	72°36½′
o $10\bar{1}2$	2 faces	29 54	57 39

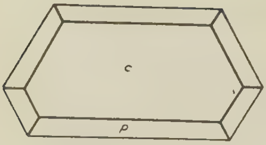

1

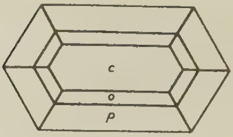

2

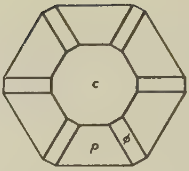

3

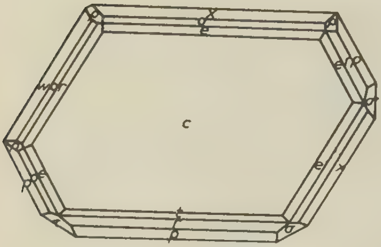

4

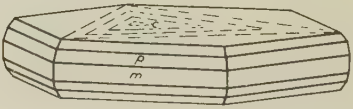

5

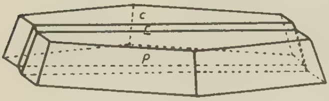

6

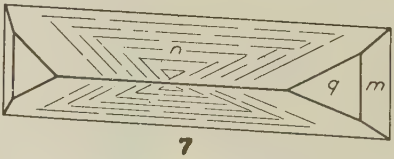

7

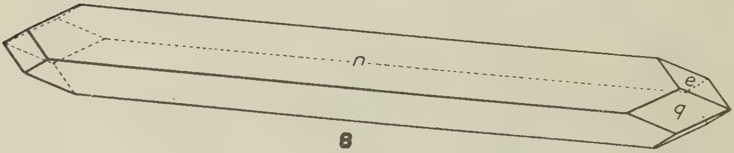

8

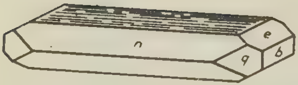

9

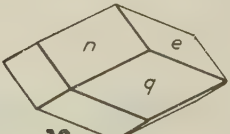

10

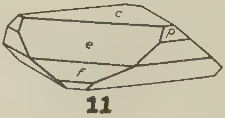

11

FIG. 1. Plan of graphite crystal from Sterling Hill, N. J., showing the forms $c\{0001\}$ and $p\{10\bar{1}1\}$.

FIG. 2. Plan of graphite crystal from Sterling Hill, N. J., showing the forms $c\{0001\}$, $p\{10\bar{1}1\}$ and $o\{10\bar{1}2\}$.

FIG. 3. Plan of graphite crystal from Sterling Hill, N. J., showing the forms $c\{0001\}$, $p\{10\bar{1}1\}$, and $\phi\{11\bar{2}2\}$.

FIG. 4. Plan of graphite crystal from Sterling Hill, N. J., showing irregular disposition of faces of the forms.

FIG. 5. Graphite crystal from Ticonderoga, N. Y., showing full hexagonal symmetry with the forms $c\{0001\}$, $m\{10\bar{1}0\}$, $o\{10\bar{1}2\}$ and $p\{10\bar{1}1\}$.

FIG. 6. Graphite crystal from Sterling Hill, N. J., showing the forms $c\{0001\}$ and $p\{10\bar{1}1\}$, with a twin lamella on $\{11\bar{2}1\}$. A cleavage plane below.

FIG. 7. Crystal of arsenopyrite from Sterling Hill, N. J., showing the forms $m\{110\}$, $q\{210\}$ and $n\{101\}$.

FIG. 8. Crystal of arsenopyrite from Sterling Hill, N. J., elongated on *b* showing $q\{210\}$, $e\{012\}$ and $n\{101\}$.

FIG. 9. Crystal of arsenopyrite from Sterling Hill, N. J., showing $b\{010\}$, $q\{210\}$, $e\{012\}$, $n\{101\}$ and a pseudobase due to striation.

FIG. 10. Crystal of arsenopyrite from Sterling Hill, N. J., equant, with $q\{210\}$, $e\{012\}$, and $n\{101\}$.

FIG. 11. Crystal of native arsenic from Sterling Hill, N. J., showing $c\{0001\}$, $e\{10\bar{1}4\}$, $f\{20\bar{2}1\}$, and $p\{01\bar{1}2\}$.

This crystal was the only one on which the faces of the lower end could also be measured; they were so placed as to indicate a horizontal plane of symmetry.

Forms. The base $\{0001\}$ is the dominant form on graphite from all localities. Generally it has splendent luster and is invariably used for orientation of a crystal on the goniometer. $\{10\bar{1}0\}$, the prism of first order, is very weak, rarely present as more than a line face, and often quite missing, always rough. Dipyramids of the first order determine the hexagonal outline of the scales. The forms $\{10\bar{1}1\}$ and $\{10\bar{1}2\}$ are about equally common, $\{10\bar{1}3\}$ slightly less so. The other six dipyramids are subordinate. No one of the dipyramids is complete in most cases but rarely all six faces of some one may be present. The zone of these faces is often completely striated so that a chain of overlapping signals is all that can be observed on the goniometer. Dipyramids of the second order never determine the outline of the crystal. They appear as tiny facets on the angles of the hexagonal scales or as line truncations of first order dipyramids.

Twinning. In selecting crystals for measurement, those whose base was quite free from striae were sought for. The vast majority of the crystals showed striations on the base in one, two or three directions, always in diagonal relation to the hexagonal outline. Two were measured upon which a single twin lamella traversed the crystal with a sharp plane face of the pinacoid in twin position, making an angle to the base of about 20°, as shown in Fig. 6. This corresponds to a face as twin plane of the form $\{11\bar{2}1\}$, which requires an inclination of 20°36′. A corresponding angle, 20°24′, was observed by Sjögren (1884) on a twin crystal. Another measured lamella gave an angle of 16°43′, corresponding most nearly to the form $\{44\bar{8}3\}$ as twin plane, which requires an inclination of 15°31′. Kenngott measured a face parallel to the direction of a twin lamella making an angle of 58° to the base, but it does not appear clearly from his description whether this was a face of the main crystal or was upon a twin lamella. He took it to be the former and made it his unit rhombohedron, but this angle corresponds to no pyramid in the second order series. If, however, it be regarded as a twin lamella, the angle corresponds to the position of the base when twinned on a face of $\{11\bar{2}3\}$, which requires an angle of 57°11′. In short, the twinning of graphite may be defined as on a face of a second order pyramid not well determined but most probably the form $\{11\bar{2}1\}$. It is evident that twinning on such a form would be possible on six faces of the pyramid which would have traces on the base in but three directions at 120° and could give rise to trigonal or hexagonal striations. The striae are due to gliding, as has long been recognized, and may be easily demonstrated by the slightest pressure on an untwinned crystal. Examination under the binocular of a plate deformed by pressure reveals on various parts of the surface every sort of combination of the six gliding surfaces, single lines or pairs, isosceles triangles or hexagons, so that there seems no reason to doubt the correctness of this interpretation.

Kenngott stated that all his measurements were approximate, particularly that of the form parallel to the basal striae which he took as unit rhombohedron and on which he based his element. The fact that the *c*-axis so derived is so nearly in accord with that of our position as shown on a preceding page is due wholly to chance. The following tabulation shows the angles of his three forms compared with the nearest calculated angles of the two series of dipyramids in our position.

Kenngott		Palache			
			ρ		ρ
$R=10\bar{1}1\wedge0001$	58°00′	$10\bar{1}2$	57°49′	$11\bar{2}3$	61°24½′
$\frac{2}{3}P^2=11\bar{2}3\wedge0001$	43 00	$11\bar{2}6$	42 32	$10\bar{1}3$	46 39
$2P^2=11\bar{2}1\wedge0001$	70 00	$11\bar{2}2$	70 02	$10\bar{1}1$	72 32

The agreement of Kenngott's angles with those of our first column is perfect, but the relation of his forms to the striae on the base makes it impossible to accept this agreement. His values must be compared to our second column and there the agreement is very poor. We can only blame the quality of his crystals.

Kenngott did not figure his crystals of graphite, but in Descloizeaux we find a figure drawn, as stated, from Kenngott's data. There is nothing to be found in Kenngott's paper to show that the habit of this figured crystal is true to nature. But it so happens that the crystal is drawn in the position adopted in this paper, and the relative proportions of the forms, especially of the second order pyramid, shown with three faces only since it was regarded as a rhombohedron, is strikingly like our Fig. 4. Thus, also by chance, the only figure of a graphite crystal extant is now justified by new observations.

During the progress of this study, Dr. M. A. Peacock examined the projections of some of the Sterling Hill crystals of graphite and afterwards drew up a projection, based on the elements determined by x-ray study. In this projection he introduced the lattice planes with greatest spacings which were to be regarded as probable crystal forms. The forms so indicated are the forms of Table 1 bearing the letters c, m, e, t, r, o, p, y, ρ, ϕ, and τ. The only form in his projection not found by any observer is the second order prism. Our list has, in addition, five forms d, w, x, π, and σ which are all weak and infrequently occurring.

The comparison of the completed form list with Dr. Peacock's projection, quite forgotten in the year or more during which the study has extended, revealed a parallelism so close as to seem worthy of record as an additional evidence of the correctness of the present interpretation of graphite morphology.

Paragenesis of the Sterling Hill Graphite

In May 1937 there were found on the 900-foot level of the mine at Sterling Hill, New Jersey, specimens showing an entirely new paragenesis for this locality. Samples were presented at that time to the Harvard Mineralogical Laboratory by Mr. L. H. Bauer, and repeatedly in the succeeding years the same donor has sent selections of carefully isolated crystals of the several minerals. Description of the material has been so long delayed because only recently were really decisive crystals of graphite found which finally solved the puzzle of its morphology.

The specimens consist of massive, coarsely crystalline limestone, with irregular impregnations of the following minerals: graphite, native arsenic, realgar, pyrite, arsenopyrite, diopside, and a few needles of either stibnite or a lead sulphantimonide. Since all of these minerals are set free without sensible injury by solution of the limestone in dilute hydrochloric acid, an abundance of the crystals of most of them can be obtained with ease. Arsenic, realgar and the antimony compound are quite new to the Franklin region.

The chief interest centered in the brilliant scales of graphite which were found in considerable numbers in the solution residue. The scales range in size from minute specks to plates 2 mm. in diameter and .5 mm. in thickness. The base is extremely brilliant and the edges of the hexagonal plate show many facets. The details of their crystal form have already been presented. Most of the graphite crystals are distorted, having suffered from movements in the embedding calcite which has caused the development of numerous gliding-plane twin lamellae in both calcite and graphite. Occasionally, however, the graphite has escaped all distortion or at least shows only a single twin lamella. The graphite crystals are generally quite free but may be partly embedded in arsenopyrite, in arsenic or in diopside.

ARSENOPYRITE

Next in abundance and beauty of the isolated crystals is arsenopyrite. The crystals, while minute, are of amazing brilliance and perfection of form. They present few crystal forms but range in habit from needles of hair-like fineness to stout prisms or flattened plates. In dimensions they commonly range from .5 by 1 mm. to 1 by 2 mm. They are chiefly bounded by the forms* $m\{110\}$, $q\{210\}$, $e\{012\}$, and $n\{101\}$. Of these *n* is generally largely developed and the hair-like crystals are elongated parallel to it. Commonest type has *n* and *q* alone, or with *m* as in Figs. 7 and 8, the latter an attempt to delineate the hair-like needles. By flattening parallel to one pair of planes of *n* the crystals take a platy form. Another mode of flattening is by development of a striation zone over the basal edge as in Fig. 9, producing a dull pseudobase; *e* is also common and may be equally developed with *n* and *q* as in Fig. 10. Sometimes but one face of *e* is present. There is a strong tendency for striae to form between *e* and *n* which is generally accompanied by a similar striation between *n* and *q* as shown in Fig. 7. This latter is often so deep as to eliminate the prism planes. Fig. 9 shows a rare type in which {010} truncates what is commonly an acute end.

Other forms measured on single crystals or in single faces or pairs are {610}, {430}, {111}, {113}, {416} and {212}. It is hoped that an analysis will be made of these exceptional crystals of arsenopyrite.

PYRITE

Pyrite, much less abundant in the residues than arsenopyrite, is present in model-perfect crystals of varied habit. The following combinations were noted: {100} and {111}; {120} alone and with {111}; a few very brilliant crystals showing {210}, {111}, {110} and {112}.

ARSENIC

Arsenic is present in but few grains and crystals. However, one was found to be measurable which yielded the forms $c\{0001\}$, $e\{10\bar{1}4\}$, $f\{20\bar{2}1\}$ and $p\{01\bar{1}2\}$ as shown in Fig. 11.

Realgar is in rude prismatic individuals with ragged terminations which admit of no measurement.

---

* The forms, symbols, and drawings are in the new position required by the results of the study of this mineral by Buerger (1936).

Needles of an antimony compound have been mentioned. Too little was secured to enable its satisfactory determination.

Diopside is the most abundant of the residue constituents. It forms irregular clusters of rounded crystals, white in color and identified only by its optical properties, since the crystals were too ill defined to be interpreted.

In the writer's genetic classification of the Franklin minerals (Palache, 1929) a subgroup was set up called "pneumatolytic products" which was stated to be practically confined to the Franklin deposit. This new paragenesis appears to belong to this group and extends its range to Sterling Hill.

REFERENCES

BRAGG, W. L., *Atomic Structure of Minerals*, 54 (**1937**).

BUERGER, M. J., *Zeits. Krist.*, **95,** 83 (1936).

DESCLOIZEUX, A., *Mineralogie* (**1874**), Plate 44, fig. 263, reproduced in Goldschmidt, *Atlas* **4,** Plate 61, fig. 5.

GOLDSCHMIDT, V., *Atlas der Krystallformen*, **4,** 89 (1918).

KENNGOTT, A., *Acad. Wien, Ber.* **13,** 469 (1854).

PALACHE, C., *Am. Mineral.*, **14,** 1 (1929).

SJÖGREN, H., *Ak. Stockholm, Öfv.* **41,** #4, 29 (1884).

MAKING CRYSTAL MODELS

D. JEROME FISHER,
University of Chicago, Chicago, Illinois.

ABSTRACT

Simplified directions are given based on the gnomonic projection for preparing a net to make hollow models of crystals from Bristol board, etc. The procedure is illustrated by detailed descriptions for making chrysolite and orthoclase models. It could be adapted easily to the making of mine or structure models.

In the study of morphological *crystal*lography (as contrasted to "*model*lography") it is customary for the student to prepare plan and perspective drawings, as well as to calculate the various crystal constants. In some cases this work is further supplemented by cutting a solid model.[1] The necessary apparatus to carry out this operation is rather costly. The writer has found that the preparation of a model made of Bristol board is not only a satisfactory substitute as regards the final result, but no expensive machinery is required and the process is valuable from the pedagogic point of view in clarifying in the student's mind the principles of crystal drawing. Moreover a collection of such models whose greatest dimension is 8 to 10 inches is a valuable asset for teaching purposes.

The plan neeeded to prepare a hollow model made of paper, cardboard, glass, cellulose acetate, etc., can be obtained easily from the face-poles of the standard equator gnomonic projection of the crystal. In what follows it is assumed that the reader is familiar with this projection and the method of making ordinary crystal drawings from it.[2] In this projection, planes (faces) are represented by points (face-poles) where lines normal to them from the center of the sphere (which coincides with the point of intersection of the crystal axes) pierce the projection plane. A crystal face might also be represented in this projection plane as a line formed by the intersection of the two planes, providing the face is considered to be moved parallel to itself until it intersects the center of the sphere. Such a projection is called the euthygraphic projection.[3] It has advantages over the gnomonic projection where it is desirable to show direction,[4] since a line may be represented in the euthygraphic projection by a point made where the line (moved parallel to itself till it goes through the center of the sphere) cuts the projection plane. A gnomonic projection is easily converted to a euthygraphic projection; from any given face-pole (of known ρ-angle) drop a line through the center of the projection and locate a point on this line, the other side of the center at a distance from the center corresponding to an angle of $(90°-\rho)$. The gnomonic scales of the projection protractor[5] greatly facilitate the plotting of these distances. A perpendicular to this line through this point is the required euthygraphic projection of the face in question.

---

[1] Goldschmidt, V., *Kursus der Kristallometrie*, 38–45 (1934).

Palache, C., and Lewis, L. W., A saw attachment: *Am. Mineral.*, **12,** 154–156 (1927).

Chace, A., and Kersten, H., Crystal models made on a milling machine: *Am. Physics Teacher*, **6,** 215 (1938).

[2] The method is very simply explained in the writer's article in the *Journal of Geology*, **32,** 538–542 (1924). Other elementary presentations in English include:

Porter, M. W., *Practical Crystal Drawing: Am. Mineral.*, **5,** 89–95 (1920) (reprinted in The Goldschmidt Two-Circle Method, 1921).

Barker, T. V., *Graphical and Tabular Methods in Crystallography*, 55–58 (1922).

Walker, T. L., *Crystallography*, 160–164 (1914).

McNabb, W. M., and J. W., Guide for crystal drawing: *Jour. Franklin Inst.*, **221,** 539–546 (1936).

Suppose one wishes to prepare a model of the simple chrysolite crystal of Fig. 1 which has all the forms of the orthorhombic dipyramidal class. The gnomonic projection (gnomonogram) of a part of this crystal is shown by continuous lines in Fig. 2. The plan drawing on *c* of this crystal is given in Fig. 3 by dotted lines. The continuous lines of this figure depict the appearance of one face of each form assuming the crystal to be "unfolded" so that each face lies in the plane of the paper [(001) plane of the crystal]. To prepare this it is only necessary to remember that the guide line represents the trace of the picture plane in the gnomonic projection and that the line of sight is assumed to be perpendicular to the picture plane; that is, the perspective drawing made from the gnomonic projection is orthogonal, not clinographic. The object is to picture each face as it appears looking normal to it; in short, the plane of the crystal face is to coincide with (be parallel to) the picture plane in each case. Thus the guide line used in drawing any given face is the euthygraphic projection of that face.

For drawing the *c* face then, since its pole is at the center of the primi-

---

[3] This is the same as the linear projection of Fedorow. It is not to be confused with the linear projection of Quenstedt, in which the projection plane is likewise normal to the *c*-axis, but at a point equal to minus unity on this axis if the crystal face is supposed to cut the center of the axial cross (or the projection plane may be considered to lie at the axial intersection normal to the *c*-axis while the crystal face cuts plus unity on the *c*-axis).

[4] Of course a direction may be shown in the gnomonic projection as a point, but then one must distinguish between two kinds of points: one derived as a face-normal, the other as in the euthygraphic projection. The stereographic and cyclographic projections are analogous, and their uses in solving geologic problems have recently been described by the writer in *Bull. Am. Assn. Petr. Geol.*, **22** (9), 1261–1271 (1938). Also see "Drillhole Problems in the Stereographic Projection," *Econ. Geol.*, **36**, 551–560 (1941) and the reference of footnote 5.

[5] Fisher, D. Jerome, A new projection protractor: *Jour. Geol.* **49**, 292–323 (1941) and 419–442 (see especially 317–318). See note at end of this article.

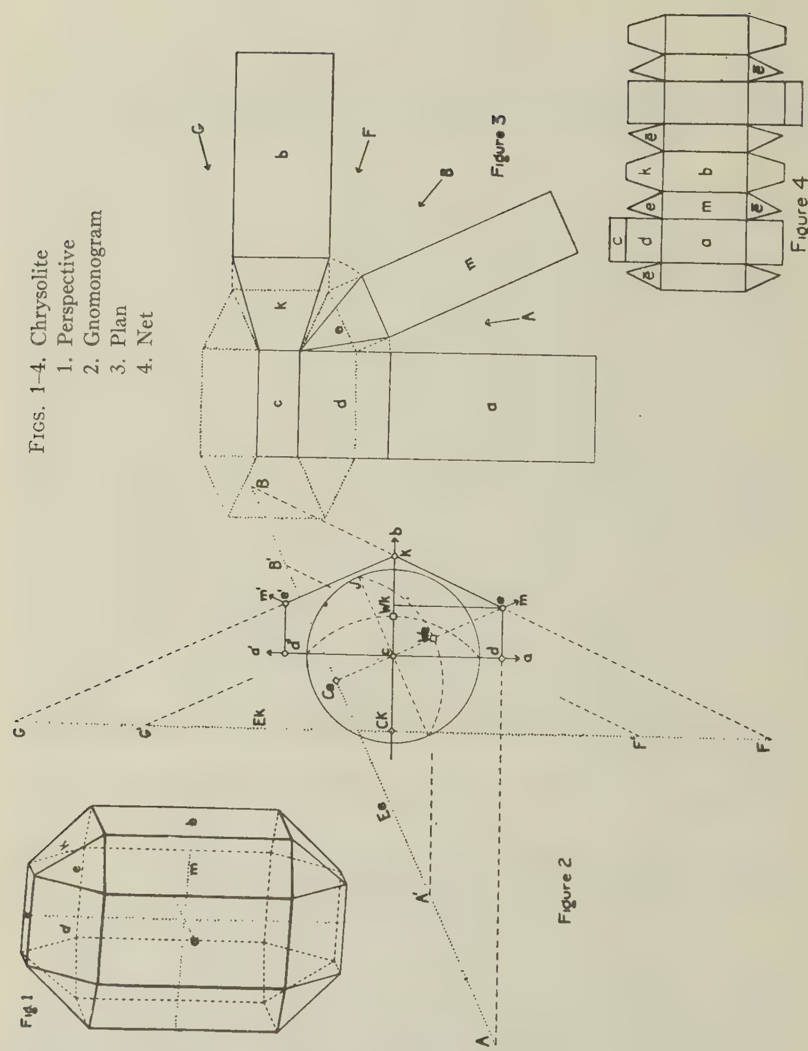

FIGS. 1–4. Chrysolite
1. Perspective
2. Gnomonogram
3. Plan
4. Net

tive circle in Fig. 2, the picture plane is horizontal (normal to the *c*-axis), the guide line becomes a circle of infinite radius whose angle point (center of the fundamental sphere rotated about the guide line as an axis into the plane of the gnomonic projection) lies at *c*. In short, the *d* edge of face *c* (that edge on face *c* made by the intersection of the *d* and the *c* faces, Fig. 3) is obtained by extending *dc* of Fig. 2 to the guide line at *a* and joining the point thus located with the angle point at *c*. Then a normal to *ca* gives the desired direction. Thus the boundaries of the face are simply normals to *cd* and *ck* of Fig. 2, drawn as in Fig. 3 with edges of lengths proportionate to those on the crystal at any desired scale of enlargement. Where the plane of projection is parallel to the *c*-face (which it is not in the monoclinic and triclinic) the ordinary plan drawing and the net drawing coincide for the *c*(001) face.

To draw face *e* of Fig. 3, go 90° from face-pole *e* of Fig. 2 along the dashed line in the direction *ec* and establish the point *Ce*, the center of the dotted zone-line *Ee*. Then *Ce* is out from *c* by $r \tan (90° - \rho)$ of face-pole *e;* thus *Ce* is quickly located with the projection protractor.[6] *Ee*, the euthygraphic projection of *e*, is normal to *ce* and serves as the guide line in drawing face *e*. Establish its angle point *We* on the central *ce* by using the stereographic scale of the projection protractor, remembering that *c* to *We* in stereographic degrees equals *ce* in gnomonic degrees.[7] The direction of *A* of Fig. 3 is the *d* boundary of face *e* and is normal to a line (not drawn in Fig. 2) joining *A* and *We*. *A* of Fig. 2 is on *Ee* where a line through *de* cuts *Ee*.[8] Similarly *B* of Fig. 3, the direction of the *k* edge of face *e*, is normal to the line *B* to *We* of Fig. 2, in which *B* is on *Ee* where cut by *ek* extended. The other edge of *e* (Fig. 3) is normal the central *Ce* to *e* of Fig. 2, since *em* extended cuts *Ee* at *Ce* and *We* lies on this line. It is drawn at such a distance from the top vertex of the face *e* as to preserve the average dimensions of the crystal being reproduced, on the same scale of enlargment as already used in drawing face *c*. This means that it is of the same length as the corresponding edge shown by a dotted line in the plan drawing on (001).

The general rule for drawing the net plan of any crystal face is to find its guide line taken as its euthygraphic projection *E*. Considering this line as a zone line, determine its angle point *W*. Find the point where a line joining the gnomonic projection (face-poles) of the two crystal faces which make the edge in question cuts the guide line *E*. Lay a straightedge on this point and *W* and using a right-angle triangle obtain the normal which is the direction desired.

---

[6] Since *J* is the angle point for the line *ce*, if one has no projection protractor the point *Ce* may be located by laying off a normal to the line *eJ* at *J* (not drawn in Fig. 2).

[7] In the absence of a projection protractor, *We* may be located by striking a circular arc with center at *Ce* and radius *Ce* to *J;* note *J* is where a line through *c* parallel to *Ee* cuts the primitive circle.

[8] Where no faces parallel to the *c*-axis are involved, paper may be saved by establishing a point *A′* on *Ee* where a line parallel *de* through *We* cuts *Ee*, and taking for the required direction a line normal to *A′ c*.

For face *m* the guide line runs through *c* normal to the *m*-arrow (e.g., it is *cJ*) and the angle point *Wm* (not indicated in Fig. 2) lies where this arrow cuts the fundamental circle. To get the *e* edge of *m*, note that a line through the *e* and *m* face-poles cuts this guide line at *c;* thus a normal to the *m*-arrow gives the desired direction, while lines parallel this arrow give the *a* and *b* boundaries of this face (this latter direction is normal to the guide line for the *m* face). The length of this face is made proportionate to the size of the face on the crystal as already outlined.

The *a*, *b*, *d*, and *k* faces are prepared in similar fashion, but the *e* length of the *d* face is made equal to the *d* length of the *e* face, and the length of the *e* edge of the *k* face is analogously determined, as shown by the two dashed-line circular arcs of Fig. 3 with centers at the top vertex of *e*.

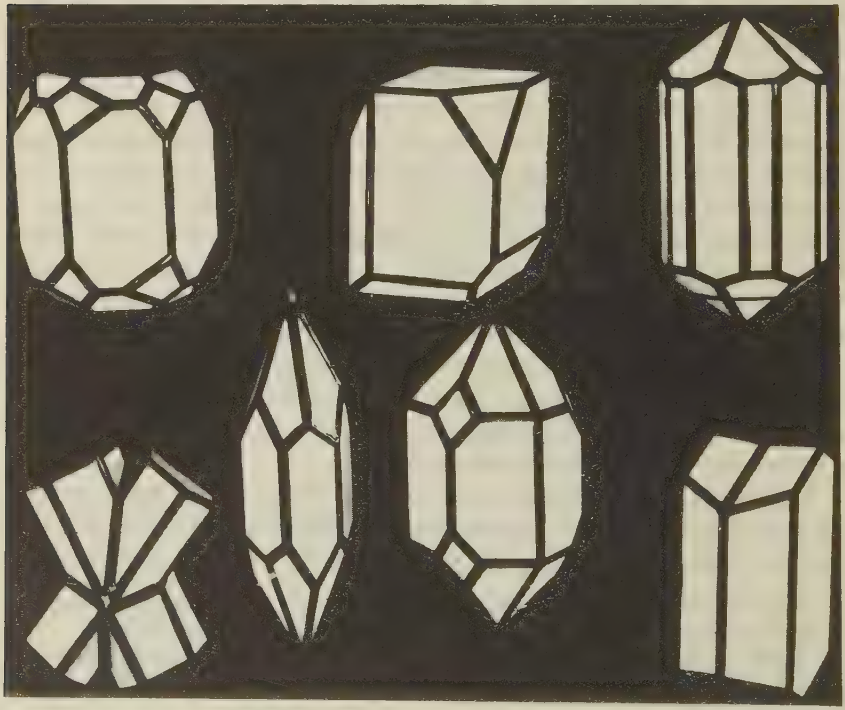

Fig. 9. Crystal Models. Vanadinite (C. G. Johnson), Kyanite (P. Herbert), Apatite (G. W. Sandberg), Staurolite (N. A. Riley), Calcite (A. Swineford), Quartz (G. Botero), and Albite (K. L. Cook).

The dashed lines continuing the edges of the [001]-zone (*m* and *b* faces in Fig. 3) make clear the relation between the plan drawing on *c* and the method of drawing here described.

To prepare the idealized model net shown in Fig. 4 a drawing is needed (in Fig. 3) for but one face of each crystal form present. This part of the task is relatively simple for a model of high symmetry consisting of but a single (closed) form. Place tracing paper over (or a sheet of wrapping paper under) Fig. 3 and with a needle prick through the corners of faces *c*, *d*, and *a*. Then move the tracing paper so that its *m* edge of *a* lies above the *a* edge of *m* of Fig. 3 and prick the corners for *e* and *m*. Proceed in similar fashion till all the crystal faces are outlined on the tracing paper. Note that the latter must be turned upside down in locating the vertex of the four faces marked $\bar{e}$ in Fig. 4. Now very carefully check the whole net for accuracy, using a T-square, right-angle triangle, and dividers or compass. Finally, place this over a sheet of Bristol board and prick all the corners through it and outline the net on the Bristol board with a sharp hard pencil as shown in Fig. 4.

The next four paragraphs are devoted to the technique of preparing a similar net for a monoclinic crystal. Following this, the method of fabricating a model from a net is described.

For the benefit of beginning workers the same method is applied to a slightly more complex case as is illustrated in Figs. 6, 7, and 8. The crystal is orthoclase from near Ontario, Oregon, collected by W. R. Lowell, perspective of which is given in Fig. 5, with forms $b\{010\}$, $c\{001\}$, $m\{110\}$, $y\{\bar{2}01\}$, and $o\{\bar{1}11\}$. The plan drawing on a normal to [001] is shown by dotted lines in Fig. 7; gnomonic and euthygraphic projections of one face of each form appear in Fig. 6. What follows is according to the rules given five paragraphs back. Let *D* of Fig. 7 which represents the highest point of the crystal (*c*-axis vertical) be common to the plan on the normal to [001] and the analogous point of the net pattern. Draw *DA* (the *o* edge of face *c*) of Fig. 7 normal to the line from *A* to *Wc* of Fig. 6. Ordinarily the *c*-face would be completed at this stage, as the general rule of finishing one face at a time is a good one. But since the length of *AB* [which $= AC = A'C' = A'B'/\cos(90° - \beta) = A'B'/\sin\ \beta$] is easily determined graphically from the length of *AC*, one side of the *b*-face, this latter face is completed first. From *A'* of the plan drawing of Fig. 7 draw *A'C'* and *A'F'* normal to the lines *Wb* to *c* and *Wb* to *F* respectively of Fig. 6, locating *C'* and *F'* of Fig. 7 by lines through *B'* and *E* normal to *Eb* of Fig. 6. Then in Fig. 7 draw *AC* and *AF* parallel and equal in length to *A'C'* and *A'F'*, respectively. Draw lines normal to *Eb* of Fig. 6 through *C* and *F* of Fig. 7, making *CG* of length appropriate to the crystal, and complete face *b* by lines parallel and equal to *AC* and *AF*. Locate *B* by making *AB* equal in length to *AC*. Draw *BH* normal to the line *H* to *Wc* of Fig. 6 locating *H* directly below *D* (in a direction parallel the *a*-axis trace of Fig. 6), and complete face *c* of the net pattern of Fig. 7 by parallel and equal lines to the three already drawn.

Face *o* of Fig. 7 is begun at *D*, making *DN* equal to *DA* and normal to the line *N* to *Wo* of Fig. 6. *NP* of Fig. 7 is made equal to *AF* and is normal to the line *P* to *Wo* of Fig. 6. *PR* of Fig. 7 is parallel to *DN*, and *DR* is normal to the line *R* to *Wo* of Fig. 6 (*R* is off the paper here; the direction *R* to *Wo* marked on Fig. 6 is obtained by placing the paper on a large sheet and extending the lines *Eo* and *yo*). *DT* and *DT′* of the *y* face of Fig. 7 (which is a rhombus only 43′ off a square) are made equal to *DR* and are drawn as normals to the lines *Wy* to *T* and *Wy* to *T′*, respectively, of Fig. 6.

Draw face *m* of Fig. 7 beginning at *B* and making *BK* of length equal *BH* and normal to the line *K* to *Wm* of Fig. 6. *BL* of Fig. 7 is made equal to *CG* and (like *KM*) is drawn normal to *Em* of Fig. 6. *LK′* of Fig. 7 is made equal to *RP* and is drawn normal to the line *K* to *Wm* of Fig. 6. This is because it is an edge between *m* and a *lower* face whose face-pole is marked by the dot in a tiny triangle[9] labelled *o′* in Fig. 6; but when one wants a lower edge like this, one uses the opposite face-pole represented by a dot in a tiny circle (marked *o″* in Fig. 6) as if the face-pole in question were operated on by an inversion (center of symmetry).[10] Similarly *K′M* of Fig. 7 is found to be equal to *DT* and is made normal to the line *M* to *Wm* of Fig. 6 (*M* is where the *m*-arrow through *y* cuts *Em*).

A net may now be prepared from Fig. 7 as was done from Fig. 3. The result is shown in Fig. 8. Specific rules that will apply to all crystals can hardly be stated. In general, the net is "strung along" some pronouncedly prismatic zone involving maximum face areas and edge lengths. The *mb*=[001] zone used in Fig. 8 could nearly as well be replaced by a *cmo*=$[\bar{1}10]$ zone. In any case great care must be exercised to keep corresponding edges of equal lengths. It will be noted that the tracing paper must be turned upside down on Fig. 7 in taking off the faces of Fig. 8, indicated with a bar over the letter. Faces such as *c* and *y* of Fig. 7, or *a*, *b*, *c*, *d*, and *m* of Fig. 3, which have a two-dimensional symmetry of two mutually-perpendicular planes plus inversion or a 2-fold axis, can be traced off in four ways (tracing paper either side up, and at 180°-azimuth

---

[9] Symbolism and method of projection used here are as described in Fisher, *op. cit.*, *Jour. Geol.* **49,** 313–319 (1941).

[10] These principles are important in preparing a net for a hemimorphic crystal, such as tourmaline, where the lower half (faces designated by face-poles placed in tiny triangles) will be different from the upper half. Here follow these rules, using a tiny circle face-pole diametrically opposite the given tiny triangle one, and then remember that the directions obtained will be those of the face opposite to the one desired; thus the face in question will appear to be upside down.

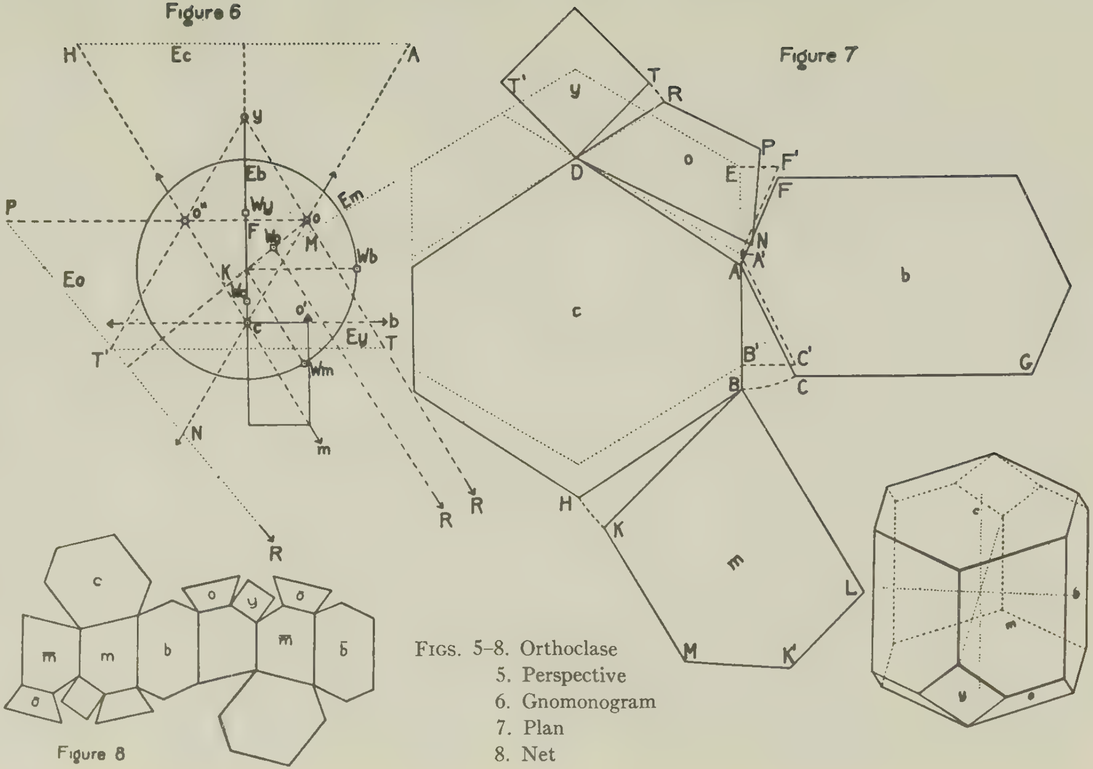

FIGS. 5–8. Orthoclase
5. Perspective
6. Gnomonogram
7. Plan
8. Net

positions in either case). Those as *k* of Fig. 3 with only one plane of symmetry can be traced off in but two ways (tracing paper either side up). Those with but inversion or a 2-fold axis, such as *b* of Fig. 7, can also be traced in but two ways (tracing paper at two azimuths 180° apart, but only one side up). Finally, those with no symmetry, such as *e* of Fig. 3 and *m* or *o* of Fig. 7, can be taken off in only one position of the tracing paper.

When ready to make the model, carefully trim off the net drawn on Bristol board (Figs. 4 or 8) along the outside lines, using a safety razor blade mounted in a convenient handle, either freehand or running against a steel straight-edge. Then lightly cut along all other lines and fold the Bristol board along these cuts. With the aid of a roll of $\frac{3}{8}$ or $\frac{1}{2}''$-wide red Scotch cellulose tape (like that used for binding lantern slides) the proper edges may now be joined together. It is important that the tape be bisected lengthwise by the crystal edge it joins. The faces may be labelled or lettered as desired. Colored or white tape, or Bristol board, may be used to give different effects as is common in model making. Two coats of colorless hard varnish improve the final product. Or shellac may be sprayed on; but do not use this as a first coat if any material in colored India ink is on the model; the ink will run.

In Fig. 9 appears a few of the 19 models made by the writer's students during the past three years. The interfacial angles are in most cases accurate to within 1°, which is far better than is true for the ordinary wooden model. At present a model is being made to show the seven type forms for each crystal class of not-too-high symmetry.

Nets of the type here described have been printed on paper to be pasted on cardboard and made by students into small models.[11] Jordan recommends washing with a weak solution of isinglass before varnishing. This is not satisfactory on Bristol board since it causes warping.

The method of model making herein described is very direct and involves no new theory.[12] The stereographic-cyclographic projections[13] may be used for the same purpose with economy of paper; the time saved in most cases seems to justify the preference for the gnomonic, however.

NOTE

The projection protractor mentioned in footnotes 5 to 7 can be obtained from the University of Chicago Bookstore, which also sells reprints of the article describing its use, as well as Penfield protractor paper.

---

[11] Jordan, J. B., *Crystallography: a Series of Nets* (1921).

Smithson, F., *Patterns for the Construction of Crystal Models*, D. Van Nostrand Co. (1928).

Barker, T. V., *The Study of Crystals*, 41–47 (1930).

[12] That is, it follows from the general theory of crystal drawing from the gnomonic projection. This is given in brief by Professor Charles Palache (*Am. Mineral.*, 5, 96–99, 1920) who kindly made several suggestions which are incorporated into this paper.

[13] Tertsch, H., *Das Kristallzeichnen auf Grundlage der stereographischen Projektion*, 18–20 (1935). Here the angles of the (010) face are wrong.

ORIGIN AND GEOMETRIC FORM OF CHALCEDONY-FILLED SPHERULITES FROM OREGON*

CLARENCE S. ROSS,
U. S. Geological Survey, Washington, D. C.

Chalcedony-filled nodules, with interesting geometric forms, are finding their way into numerous mineral collections. Central Oregon is the outstanding producer of these specimens, but similar ones come from Nevada and California. Dake[1] has described the Oregon specimens as follows:

> The Central Oregon district has produced many thousands of these agate-filled nodules. Madras seems to be the center of production, but choice specimens are also found on the Warm Springs Indian Reservation in Wasco County. The area south of Antelope is also a good producer. The nodules, also known as "Thunder Eggs" . . . , seem to be associated only with rhyolitic rocks, . . . Generally the nodules have an average diameter of about six inches, although they are found in perfect specimens as small as one-fourth of an inch and as large as three feet in diameter, all alike in exterior and interior appearance. . . .
>
> . . . Only about one out of five will prove an outstanding specimen, the others will be only mediocre. . . . The nodules appear to occur in lenses or "beds," probably in areas where the lavas were especially vesicular, presenting numerous cavities where deposition could take place. . . .
>
> . . . Each locality appears to produce a distinctive type of nodule, instantly enabling experts to distinguish them as such. However, no two specimens are exactly alike in the interior colorings, markings, and patterns.

Recently, General J. S. Hatcher, an enthusiastic mineral collector, kindly presented a number of very fine specimens of the nodules for use in detailed study; and those illustrated in Plate 1 were cut and polished by him.

The great interest in the Oregon material has heretofore been as mineral specimens, showing striking geometric forms, but they are also outstanding in the detail of geologic history that is presented. The most interesting geometric forms assumed by the chalcedony fillings are five-pointed stars, some of which are very perfect. Two of these are illustrated in Plate 1, that in Fig. (*c*) having been cut nearly across the laminae of the chalcedony, and that in Fig. (*b*) roughly parallel. Those cut across the bedding make the most beautiful specimens but the position cannot be determined in advance of cutting. Figure (*d*) represents a filled cavity with roughly square outline.

The geometric form of a filled cavity which will give a five-pointed star in cross section presents an interesting problem. Any gas cavity which forms in a homogeneous medium will tend to have a symmetrical and

---

* Published by permission of the Director, U. S. Geological Survey.

[1] Dake, H. C., The gem minerals of Oregon: *Oregon State Dept. of Geol. and Mineral Industries*, Bull. **7**, 1–16 (1938).

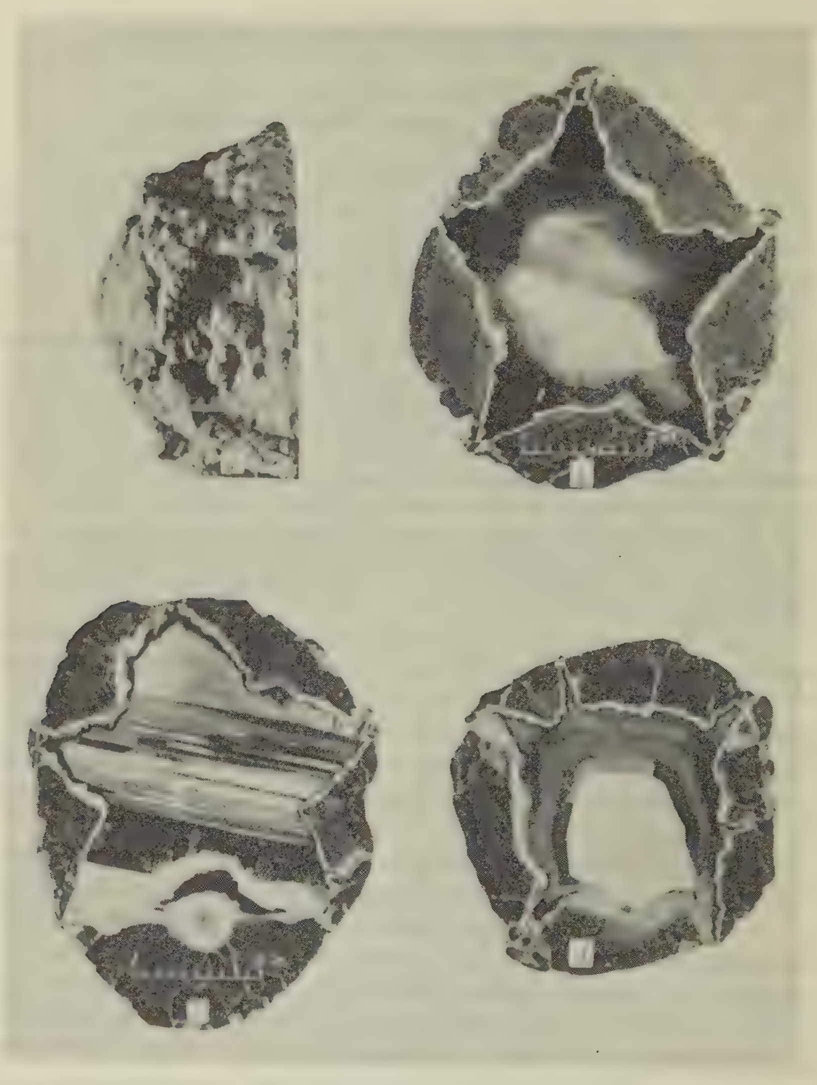

PLATE 1

FIG. (*a*) Exterior of filled vesicles represented in figure (*b*). Shows the cauliflower-like form assumed on the contact between devitrified and glassy material. Note ridges corresponding to points of star in (*b*). $\times\frac{2}{3}$

FIG. (*b*) Chalcedony-filled vesicle cut nearly parallel to lamination of the chalcedony. Gray outer portion is devitrified welded tuff. $\times\frac{2}{3}$.

FIG. (*c*) Chalcedony-filled vesicle cut across lamination in chalcedony. $\times\frac{2}{3}$.

FIG. (*d*) Chalcedony filling representing a roughly cubic vesicle. $\times\frac{2}{3}$.

equidimensional geometric form. With small cavities or in a medium that is not too viscous, the cavity will tend to have a spherical form. However, when the cavity is large and especially where it develops in a highly viscous or almost solid glass, the force required for spherical expansion is very great. In such a medium, expansion by rupture or tearing will require very much less energy, and the rupture planes will tend to symmetrically enclose the cavity developed.

Wright[2] has described hollow lithophysae from Iceland as follows:

> The cavities are in the shape of a cube about 25 mm. on a side. . . . The inner walls are not perfectly flat, but show strong diagonal ribs passing from one corner of a cube face to the opposite corner, as though each cube face had not been quite fully developed into a plane, but still has superimposed on it four negative triangular tetrahexahedral faces, each four-sided pyramid thus formed points toward the center of the cube and not away from the center, ... The fact that any irregularity on the one face finds its counterpart on the face adjacent to it and intersecting it at the edge of the cube proves that the faces were originally together and were gradually forced apart as crystallization proceeded. . . .

We may picture a cube as developed from six four-sided pyramids bounded by rupture planes, and with their apices meeting at the center. There will be 12 triangular planes (the planes of rupture), extending from the center to the 12 edges of the cube. If such a system of ruptures developed without expansion there would be six four-sided pyramids, their apices meeting at the center and their bases corresponding to the six sides of the cube. However, expansion of the gas cavity and rupture proceed together and the effect is as if the apices of the pyramids were pushed toward their bases with a flattening of the pyramid. In some instances a nearly cubic cavity is produced, but with each face marked with four triangles that represent traces of the rupture planes. In others, there remains a flattened pyramid projecting inward from each side of the cube (i.e., a negative tetrahexahedral pyramid), and the resultant form resembles the well-known hopper shaped halite crystals.

In some of the filled cavities from Oregon, the geometric form is roughly that of a cube, as shown in Plate 2, Fig. (*d*); but the star-shaped forms are sections across a modified pyritohedron, each of whose 12, 5-sided faces is represented by an inward projecting pentagonal pyramid. The form was produced by 30 triangular shear planes extending from the center and terminating at the edges of the 12, 5-sided faces along which shear occurred. Expansion, in effect, pushed the resulting apices of these pyramids toward their base (the faces of the pyritohedron), but not sufficiently far enough to eliminate the negative pyramid. Such a figure will give a 5-pointed cross section when cut in a number of directions,

---

[2] Wright, Fred E., Obsidian from Hrafntinnullryggur, Iceland, its lithophysae and surface markings: *Geol. Soc. Am. Bull.*, **26,** 255–286 (1915).

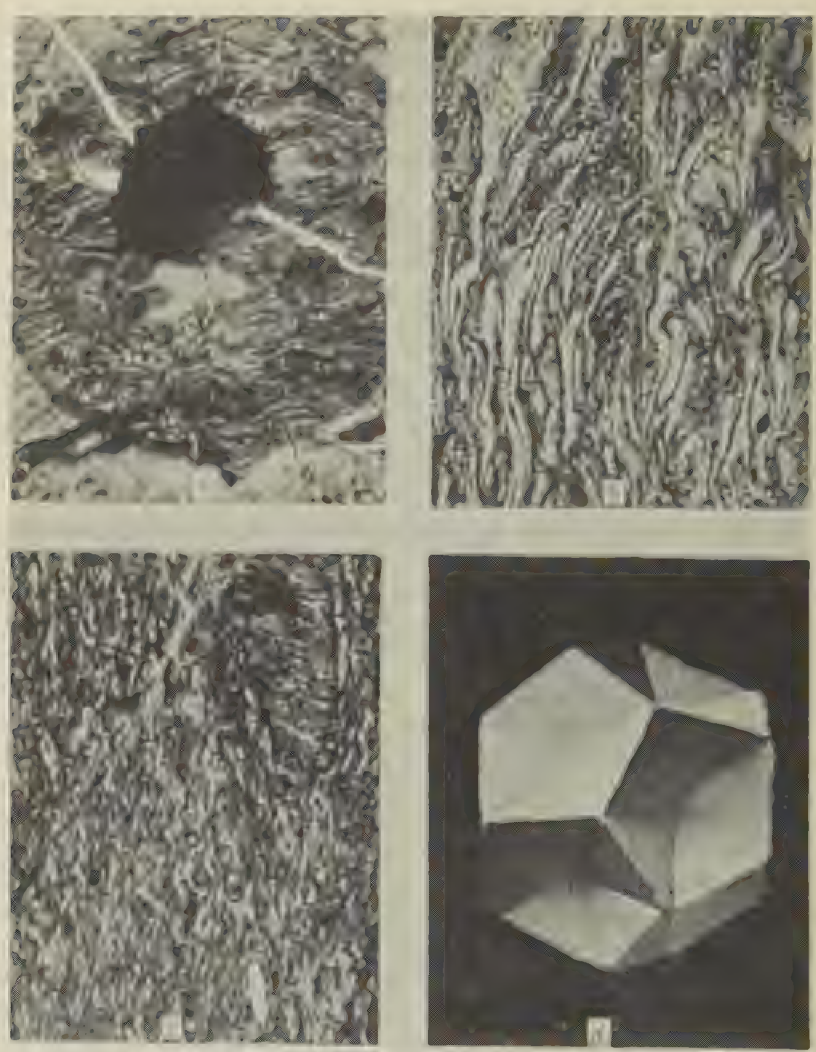

PLATE 2

FIG. (*a*) Spherulite from welded tuff, American Falls, Snake River, Idaho, showing similarity to Oregon spherulites. Central area (black) represents a nearly circular cavity; dark gray zone is devitrified glass (feldspar + cristobalite), and the light gray portion at the bottom of the figure is glass. Shard structure shows in the devitrified portion. ×48.

FIG. (*b*) Shard structure in material surrounding chalcedony in Plate 1, Fig. *b*. Fine grained diagonal structure crossing shards is composed of the radial feldspar-cristobalite aggregate. ×54.

FIG. (*c*) Tuff structure as in (*b*) but with older tuff fragment near upper right corner. ×12.

FIG. (*d*) Model of the form of the cavity giving the star-shaped chalcedony fillings. A shallow negative pyramid marks each of the 12 pentagonal pyritohedral faces.

the most perfect star being given when the cut is made about one-third above or below the equator of the spherical mass. Of course, the geometrically perfect figure outlined here will be produced only under ideal conditions. In nature there will be various modifications, and distortions due to a lack of homogeneity of the enclosing media will modify or destroy the ideal symmetry. However, the perfection of some of the stars shown in cross section indicates a close approximation to the ideal form.

In some of the nodular masses, the boundaries between the twelve pseudopyritohedral faces are marked by irregular ridges on the outer surface and these outline 12 approximately equal areas, in some of which a roughly pentagonal shape is observable. Such ridges and one-half of such a pentagonal area is illustrated in Plate 1, Fig. (*a*). The ridges are also represented by the small protuberances at each star point in Fig. (*b*).

The material surrounding the chalcedony is gray-brown in color and without structure visible to the eye, but thin sections show that this is composed of welded tuff fragments as illustrated in Plate 2, Figs. (*b*) and (*c*). The tuff structure is very perfectly preserved despite distortion and flattening due to elimination of interstitial pores and subsequent crystallization. Near the center of the figure are several shard structures that are folded back on themselves as a result of compression of fragments that were originally *Y* shaped, being formed by the walls between three adjacent bubbles. The fine-grained pattern that extends diagonally across the figure represents the radially fibrous structure of the spherulite. Figure (*c*) shows a small fragment of an earlier welded tuff enclosed in the younger one, and a number of such enclosed fragments occur in each slide studied. The radial structure of the spherulite extends without interruption across the older fragment, showing that devitrification was subsequent to consolidation.

A glassy volcanic ash evidently fell in so hot and plastic a condition that welding was complete and a nearly homogeneous material was produced, but even after this it retained volcanic gases in solution in the glass. These gases began to collect locally at centers of crystallization and, as crystallization proceeded, more and more gas collected and enlarged the cavity. This crystallized portion is made up, as is usual in such spherulites, of radial aggregates of feldspar and cristobalite, and the outer boundary of the spherulites has a cauliflower-like habit although roughly spherical in shape. Thus the nodules represent hollow spherulites that were subsequently filled with chalcedony. The material enclosing the crystalline spherulites has entirely broken down, and as it is reported to be a clay, it is probably a bentonite, that is, an alteration product of glass. The part that crystallized resisted weathering and lies imbedded in clay.

Material similar to the devitrified, welded tuff from Oregon is illustrated in Plate 2, Fig. (*a*). This is from American Falls, Snake River, Idaho, and has been described by Mansfield and Ross.[3] This specimen shows the central cavity; a nearly circular area of enclosing material, composed of radial aggregates of feldspar and cristobalite; the whole enclosed in glass that is still fresh.

The following geologic history is, therefore, revealed by the Oregon "thunder eggs." Explosive volcanic activity produced finely divided glassy ash, which fell in a hot plastic condition that permitted its rewelding into a homogeneous material. While still hot, local centers of crystallization were set up, around which spherulitic masses of intergrown cristobalite and feldspar were formed. The formation of these anhydrous minerals released volatiles originally in solution in the glass. The gradual collection of volatiles exerted a pressure, which combined with the cooling shrinkage of the enclosing material, forced the walls of the cavity outward, expansion being by rupture along symmetrically arranged planes. The more perfect of these cavities had the geometrical symmetry of a modified pyritohedron bounded by 12 inward projecting, 5-sided pyramids, formed by the shear along 30 triangular planes. The resultant cavity was later filled by chalcedony that was probably deposited during the alteration of the enclosing material to a clay.

---

[3] Mansfield, G. R., and Ross, C. S., Welded rhyolitic tuffs in southeastern Idaho: National Research Council, *Trans. Am. Geophysical Union*, Part **I**, 308–391 (1935).

NOTES AND NEWS

CALCITE CRYSTALS WITH RHOMBOID TUBES FROM GUANAJUATO, MEXICO

Charles R. Toothaker,
Commercial Museum, Philadelphia, Pennsylvania.

In 1892 or 1893 a small lot of calcite crystals of unusual form was collected by Dr. A. E. Foote at Guanajuato, Mexico. There were less than fifty of these crystals and because they were so few and so peculiar in development it may be safely assumed that they all came from one cavity or pocket. In outward appearance these crystals are seemingly oblong prisms, terminating in curved faces which come to a rather sharp point. If it were not evident at once that the mineral is calcite, it could easily be mistaken for a monoclinic substance, elongated parallel to the *a* axis, with a vertical plane and a twofold axis of symmetry. This oblong prism is bounded by two faces which are not smooth planes but are composed of many slightly curved, bright surfaces which give these faces a somewhat mottled appearance, and by two other faces which are invariably narrower and consist entirely of striations which run in the long direction of the crystal.

The cleavage at the base of the crystal and the incipient cleavages which show on it, furnish an easy clue to the direction of the crystal axes. The two wide faces of the oblong prism seem to be an attempt to form the negative rhombohedron *r*. Mr. Gordon's measurements, however, show it to be an oscillatory combination of $e\{01\bar{1}2\}$ and $\epsilon\{01\bar{1}1\}$. Some crystals show very definitely three bright faces of the negative rhombohedron $(01\bar{1}2)$. These faces are truncated by a basal plane *c* which, as is usual on calcite, is rather rough. A negative rhombohedron $f\{02\bar{2}1\}$ is well developed on two rhombs on one specimen.

The striations, which form the narrower sides of the oblong prism are composed of oscillations of $v\{21\bar{3}1\}$ and $v\{21\bar{3}\bar{1}\}$. Nearly all the crystals show small, smooth faces of $M\{40\bar{4}1\}$.

The curved, four-sided point of the prism, fairly smooth and reasonably brilliant, seems to be a combination of the negative rhombohedron *f* influenced by what Mr. Gordon calls a doubtful form $\{2.10.\overline{12}.1\}$.

In outward shape these crystals are very unusual. However, they were figured by O. Mügge (*Neues Jahrb. Min.*, 76–78, 1897). Unfortunately, he did not show the terminations. Mr. Gordon thinks Mügge may have been in error in his drawing since he attributes the striations to oscillation of $\{\bar{1}102\}$ with $\{21\bar{3}1\}$ and $\{21\bar{3}\bar{1}\}$, whereas all the available crystals (eight or more) show the oscillation to be between $\{21\bar{3}1\}$ and $\{21\dot{3}1\}$.

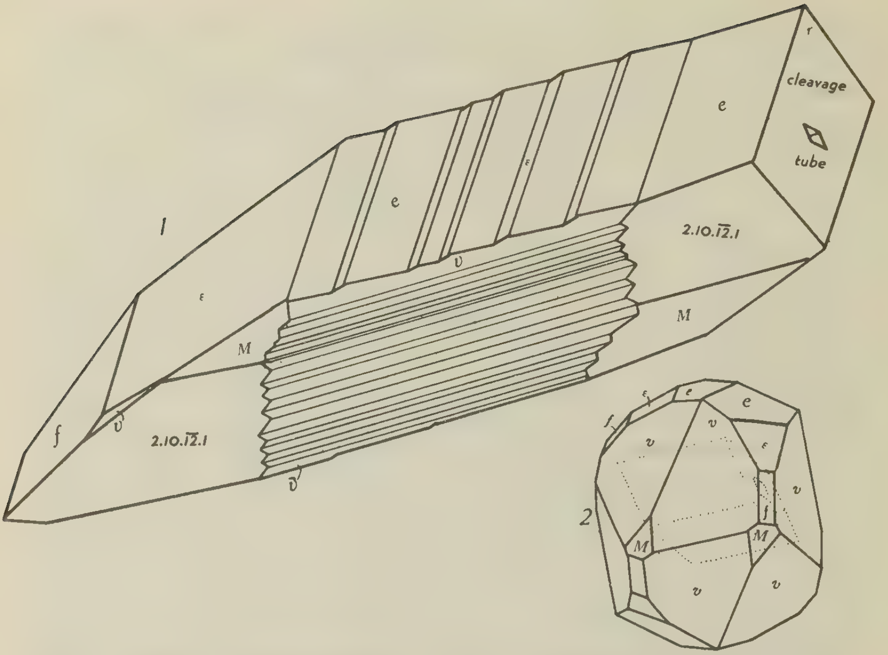

FIG. 1. Drawing of crystal by Samuel G. Gordon, showing forms which he measured.

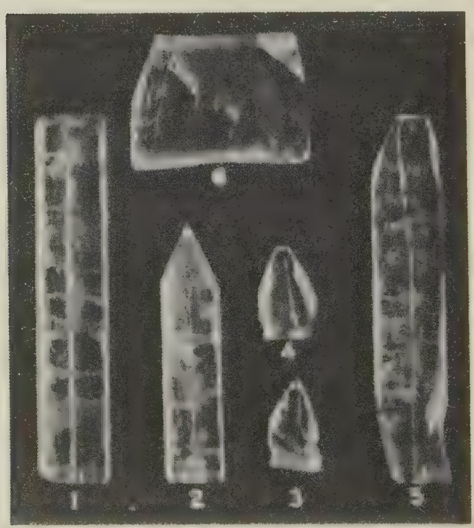

FIG. 2. Calcite from Guanajuato, Mexico, showing rhomboid hole as a white line. Nos. 2, 3 and 4 show terminations.

The most remarkable feature about these crystals is that each shows a white line running lengthwise through its center (Fig. 2). This white line follows a direction which would be the intersection of two cleavage planes. It is parallel to the four sides of the oblong prism. In reality the white line is an open hole, or tube, through which a hair or fine wire can be passed. This hole is rhomboidal in shape and its four surfaces are two planes of the unit rhombohedron *r*.

When a hole approaches the end of a terminated crystal, it gradually becomes smaller and finally apparently closes. The rhomboid hole described can be considered a negative crystal. The peculiar feature is that it is found in every crystal of this small lot collected at Guanajuato more than forty-five years ago, and that it invariably follows the same crystallographic direction.

Certain flattened quartz crystals from Hot Springs, Arkansas, also collected by Dr. A. E. Foote about the same year, show a distinct white line running through them. This white line, however, is not an opening and follows in a general way the direction of the vertical axis of the crystal. There seems to be at least an outward similarity in the distortion and in the formation of a white, seemingly axial line.

Specimens were sold by Dr. Foote to Clarence S. Bement (six of which are in the American Museum of Natural History, New York); to George Vaux, Jr.; to the Vaux collection of The Academy of Natural Sciences, Philadelphia, and probably to a few other collectors.

The writer is deeply indebted to Mr. Samuel G. Gordon of The Academy of Natural Sciences of Philadelphia for accurate crystallographic measurements, the determination of the crystal forms and for the drawing which accompanies this article (Fig. 1).

Professor Norman L. Bowen of the University of Chicago was the recipient of the honorary degree of Doctor of Laws at the Centenary celebration of Queens University, Canada, October 17, 1941.

Dr. Bowen has also been awarded the Penrose Medal by the Council of the Geological Society of America "in recognition of his achievements in the application of the principles of physical chemistry to the study of the origin of igneous rocks." The presentation will be made at the annual meeting of the Geological Society at Boston.

Professor Esper S. Larsen, Jr., of Harvard University has been awarded the Roebling Medal for meritorious achievement by the Council of the Mineralogical Society of America. The presentation will be made at the annual meeting of the Mineralogical Society at Boston.

INDEX TO VOLUME 26

Leading articles are in **bold face** type; notes, abstracts and reviews are in ordinary type. Only minerals for which definite data are given are included in the index.

Abkhazite (Efremov)............ 349
Adularia, linear thermal expansion of. (Rosenholtz, Smith)...... 391
Aikinite........................ 27
Alexander, A. E. Closer inspection of industrial diamonds prior to use advocated.............. 347
Allanite (analysis)............... 114
Alluaudite...................... 682
Amphibole (optical data)..639, 640, 641
Analcite, sedimentary. (Ross)..... 627
Andersen, O. Memorial of W. C. Brögger.................... 167
Apatite crystals with colored cores in Victorian granitic rocks. (Baker).................... 382
Apophyllite, skeletonized, from Crestmore and Riverside, Calif. (Bailey).................... 565
Arite, nature of. (Holmes)........ 198
Armenite. (Neumann)........... 235
Arrojadite. (Mason)............. 681
Arsenic and arsenopyrite, morphology of. (Palache)........ 709
Australasian Antarctic Expedition; Scientific Reports. Vols. III, IV. [Book review]........... 454

Babingtonite from Quabbin Aqueduct, Mass., occurrence and origin of (Schaub)........... 121
Bagrowski, B. P. Pyrope garnet vs. ruby spinel in Kansas.... 675
Bailey, E. H. Skeletonized apophyllite from Crestmore and Riverside, Calif.................. 565
Baker, G. Apatite crystals with colored cores in Victorian granitic rocks............... 382
Bannister, F. A................. 631
Barbertonite (new mineral)....... 311
Barnes, V. E................... 194
Bassetite (Meixner)............. 235
Bates, J. D., with Pegau, A. A. Some little known minerals of the Bear Mt. section of the Hudson Highlands.......... 673
Bell, J. F. Morphology of mechanical twinning in crystals...... 247
Belyankin, D. S. and Petrov, V. P. Grossularoid group-hibschite, plazolite.................. 450
Berlinite (Strunz)............... 631
Berry, L. G.................... 194
Billiet, V...................... 632
Biotites, relation between color and chemical composition. (Hall).. 29
Biotites, relation between chemical composition and refractive index. (Hall)................ 34
Biotite (optical data)..........................238, 637, 640, 641, 642
Bismite = bismoclite............. 651
Bismoclite from Goldfield, Nev. (Schaller).................. 651
Bosazza, V. L. Adsorption of malachite green by some clay minerals....................... 396
——— Occurrence of a coarsely crystalline kaolin mineral in some South African fire clays.. 290
Bradleyite, a new mineral, sodium phosphate-magnesium carbonate. (Fahey, Tunell)......... 646
Brögger, W. C., memorial of (Andersen).................... 167
Brookite space group, representatives of. (Donnay).......... 195
Brugnatellite.................. 314
Buddhue, J. D. Some soluble constituents of meteorites....... 677
Burfoot, J. D. Jr. A. C. Gill's development of concept of unique diameters.................. 617
Butler, R. D................... 194

Cahn, Lazard, memorial of. (Palache).................... 174
Cahnite. (Palache).............. 429
Calcite crystals with rhomboid tubes from Guanajuato, Mexico. (Toothaker)............ 733
Celadonite and glauconite, chem-

ical composition and genesis of. (Hendricks, Ross) 683
Cerite, Colorado. (Hanson, Pearce) 110
Chalcedony-filled spherulites from Oregon, origin and geometric form of. (Ross) 727
Chesley, F. G., with Lukesh, J. S. Graphical interpretation of cubic powder patterns 395
Chlorite, (optical data) 370
Chondrodite 674
Chrome-micas. (Whitmore) 204
Cinnabar coloration, variation in. (Dreyer) 195
Clay minerals, adsorption of malachite green. (Bosazza) 396
Clay minerals, hydrothermal formation of, in laboratory. II. (Norton) 1
Clay minerals, observations with electron microscope. (Inuzuka) 448
Cleavage flakes, optical properties of. (Taylor) 203
Clinozoisite (optical data) 370
Coloring in minerals, types of. (Kennard, Howell) 405
Columbomicrolite from Eshowe, Natal. (de Villiers) 501
Commercial Quarry, Crestmore, California, section across. (Woodford, Crippen, Garner). 351
Copple Crown-Merrymeeting Lake area of new Hampshire, igneous rocks of. (Quinn) 201
Cordierite, optic properties of, in relation to alkalies in the cordierite-beryl structure. (Folinsbee) 485
Crippen, R. A. and Garner, K. B. with Woodford, A. O. Section across Commercial Quarry, Crestmore, Calif. 351
Crystal models, making. (Fisher) .. 718
Crystallographic procedures. (Wolfe) 55
Crystallographic Society 630
Cubic powder patterns, graphical interpretation of. (Lukesh, Chesley) 395
Cuprojarošite. (Kosta) 136
Cuprokirovite. (Vertushkov) 136

Dana's Manual of Mineralogy. (Hurlbut) [Book review] 572
Davidson, H. R. Geometrical crystallography of PbO_2 and Pb_5O_8 18
de Villiers, J. E. Columbomicrolite from Eshowe, Natal 501
——— Optical properties and crystallography of zoned pumpellyite from Witwatersrand 237
Devilline 293
Diaboleite from Mammoth Mine, Tiger, Ariz. (Palache) 605
Diamond crystal, distorted. (Kraus, Slawson) 199
Diamonds for industrial purposes, cutting of. (Kraus, Slawson) 153, 199
Diamonds, industrial, inspection prior to use. (Alexander) 347
Dickinsonite, unit cell of. (Wolfe). 204, 338
Discredited species 294, 631, 681
Djalmaite, a new radioactive mineral. (Guimarães) 343
Donbassite (Lazarenko) 349
Donnay, J. D. H. 195
Dreyer, R. M. 195

Eardley, A. J. [Book reviews] 232
Efremov, N. E. 349
El Burro, Coahuila, Mexico, meteorite. (Henderson) 655

Faessler, C. 196
Fahey, J. J. and Tunell, G. Bradleyite, a new mineral, $Na_3PO_4 \cdot MgCO_3$ 646
Fairbairn, H. W. Petrofabric relations of nepheline and albite in litchfieldite from Blue Mountain, Ont. 316
Fisher, D. J. Making crystal models 718
Fluorescent sodalite and hackmanite from Magnet Cove, Ark. (Miser, Glass) 437
Folinsbee, R. E. Chemical composition of garnet associated with cordierite 50
——— Optic properties of cordierite in relation to alkalies in the cordierite-beryl structure. 485

Foshag, W. F. Problems in the study of meteorites 137
Freedman, J. 202
Frondel, C. Constitution and polymorphism of the pyroaurite and sjögrenite groups 196, 295
——— **Paramelaconite, a tetragonal oxide of copper** 657
——— **Unit cell and space group of vrbaite, seligmannite and samsonite** 25
——— **Whitlockite, a new calcium phosphate, $Ca_3(PO_4)_2$** 145, 197
——— 196, 197, 294

Garner, K. B., with Woodford, A. O. and Crippen, R. A. Section across Commercial quarry, Crestmore, Calif. 351
Garnet associated with cordierite, chemical composition of. (Folinsbee) 50
Gehlenite (optical data) 371
Geology of coal. (Stutzer, Noé) [Book review] 232
Gillespite, unit cell and space group of. (Pabst) 199
Gill's concept of unique diameters . 617
Glass, J. J. with Miser, H. D. Fluorescent sodalite and hackmanite from Magnet Cove, Ark. 437
Glauconite and celadonite, chemical composition and genesis of. (Hendricks, Ross) 683
Glauconites, New Zealand, composition and properties of. (Hutton, Seelye) 595
Gnomonic projection in the hexagonal system. (Ramsdell) 201
Godlevsky, M. N. 293
Gordon, S. G. 235, 293, 294
Graphite, morphology of. (Palache) 709
Grossularoid group: hibschite, plazolite. (Belyankin, Petrov). 450
Guimarães, C. P. Djalmaite, a new radio-active mineral 343
Gumner, W. K. 198

Hackmanite, fluorescent (analysis). 444
Hall, A. J. Relation between chemical composition and refractive index in the biotites 34
——— **Relation between colour and chemical composition in the biotites** 29
Hanson, R. A. and Pearce, D. W. Colorado cerite 110
Headdenite=arrojadite 681
Helium retentivities of minerals. (Keevil) 403
Henderson, E. P. Chilean hexahedrites and the composition of all hexahedrites 546
——— **El Burro, Coahuila, Mexico, meteorite** 655
Hendricks, S. B., and Ross, C. S. Chemical composition and genesis of glauconite and celadonite 683
Herrengrundite, identical with devilline. (Meixner) 293
Hess, H. H. Pyroxenes of common mafic magmas. Part I 515
——— Part II 573
Heterogenite; stainerite, mindigite and trieuite identical with (Billiet, Vandenriessche) 632
Heterosite. (Mason) 681
Hexahedrites, Chilean, and the composition of all hexahedrites. (Henderson) 546
Hibschite 450
Hills, E. S. Outlines of structural geology. [Book review] 232
Holmes, R. J. 198
Howell, D. H. with Kennard, T. G. Types of coloring in minerals .. 405
Hunt, W. F. [Book review] 135
Hurlbut, C. S. Jr. Dana's Manual of Mineralogy. [Book review]. 572
Hutton, C. O. and Seelye, F. T. Composition and properties of New Zealand glauconites 595
Hydrobiotite. (Ruthruff) 478
Hydrotalcite (*x*-ray and optical data) 304
Hydrothermal deposits in Specimen Mountain volcanics, Rocky Mt. National Park, Colo. (Wahlstrom) 204, 551
Hydrothermal formation of clay

minerals in the laboratory. (Norton) 1
Hydrotungstite (Kerr, Young) 199

Idocrase and scapolite from Manchester, New Hamp. (Stewart) 509
Interference figures in convergent light. (Donnay) 195
Inuzuka, H. Observation of clay minerals with electron microscope 448

Jarosite, formation of, on pyrite ornaments. (Pough) 562
Jarošite. (Kokta) 136
Jarrell, R. F. 197
Jordanite, structural cell of. (Berry) 194
Joseite from British Columbia. (Peacock) 200

Kaolin (analysis) 398
Kaolin mineral, coarsely crystallized, in S. African fire clays. (Bosazza) 290
Keevil, N. B. Helium retentivities of minerals 403
Kennard, T. G. and Howell, D. H. Types of coloring in minerals 405
Kerr, P. F. Memorial of Philip Krieger 178
——— 198, 199
Kirovite. (Vertushkov) 136
Kokta, J. 136
Kraus, E. H. and Slawson, C. B. Cutting of diamonds for industrial purposes 153, 199
——— 199
Krieger, Philip, memorial of. (Kerr) 178
Kurnakovite. (Godlevsky) 293
Kutukova, E. I. 135

Lacroix, A. 235
Lamprobolite, a new name for basaltic hornblende. (Rogers) 201
Lapparentite (of Ungemach) = tamarugite. (Gordon) 235
Lapparentite. (Rost) 236
Laumontite (optical data) 371
Lazarenko, E. K. 349
Lemnäsite = alluaudite 682
Lomerson, W. W. 198
Lukesh, J. S. and Chesley, F. G. Graphical interpretation of cubic powder patterns 395

Macdonald, G. A. Progressive metasomatism of serpentine in the Sierra Nevada of California 276
Magnet Cove, Ark., list of minerals. 133
Manasseite, new mineral. (Frondel) 310
Marie Byrd Land rocks, notes on. (Stewart) 42
Martite in micaceous hematite near Esmont, Va. (Pegau, Overstreet) 512
Mason, B. 681, 682
McConnell, D. and Pondrom, W. L. Jr. X-ray crystallography of seamanite 446
Mechanical twinning in crystals, morphology of. (Bell) 247
Meixner, H. 235, 293
Melanchlorheterosite 681
Melentiev, B. V. 135
Merrymeeting Lake area of New Hampshire, igneous rocks of. (Quinn, Stewart) 201, 633
Meteorite, El Burro, Coahuila, Mexico. (Henderson) 655
Meteorites, problems in the study of (Foshag) 137
Meteorites, soluble constituents of. (Buddhue) 677
Michell, W. D. Paragenesis of pegmatite minerals of Striegau, Silesia 262
Milner, H. B. Sedimentary petrography. [Book review] 135
Mindigite = heterogenite 632
Mineralogical Society of America
  List of correspondents, fellows, members and subscribers 208
  List of former officers and meeting places 206
  Nominations for officers for 1942. 571
  Proceedings of 21st. annual meeting 187
Miser, H. D. and Glass, J. J. Fluorescent sodalite and hackmanite from Magnet Cove, Ark. 437

Molybdenite at Magnet Cove, Ark. (Sleight) 132
Monticellite (optical data) 372
Mont Laurier-Senneterre highway, petrographic study. (Faessler). 196
Montmorillonite (analysis) 397
Murdoch, J. Pyrostilpnite from Randsburg, California 130
——— **Valentinite crystals from California** 613

Na-purpurite and Na-heterosite =pupurite+alluaudite 681
Neopurpurite=heterosite 681
Nepheline. (Winchell) 536
Nepheline and albite in litchfielite from Blue Mountain, Ont., petrofabric relations of. (Fairbairn) 316
Nephrite jade from Monterey Co., Calif. (Rogers) 202
Newhouse, W. H. 197
New minerals described:
  Barbertonite 311
  Bradleyite 646
  Djalmaite 343
  Manasseite 310
  Sjögrenite 309
  Whitlockite 145
New mineral names 135, 235, 293, 349, 456
New York Mineralogical Club 455
Neumann, H. 235
Nininger, H. H. 199
Noé, A. C. with Stutzer, O. Geology of coal. [Book review] 232
Norton, F. H. Hydrothermal formation of clay minerals in the laboratory Part II 1

Olivine and pyroxene of Mt. Tripyramid, New Hamp. (Smith). 202
Ore-bearing pipes in the Tarryall Range, Colo. (Butler, Riley) 194
Osbornite. (Bannister) 631
Outlines of structural geology. (Hills) [Book review] 232
Overstreet, W. C. with Pegau, A. A. Martite in micaceous hematite near Esmont, Virginia 512

Pabst, A. 199
Page, L. R. 200
Palache, C. Contributions to the mineralogy of Sterling Hill, New Jersey: Morphology of graphite, arsenopyrite, pyrite and arsenic 709
———**Crystallographic notes: cahnite, stolzite, zincite, ultrabasite** 429
——— **Diaboleite from Mammoth Mine, Tiger, Ariz.** 605
——— **Memorial of Lazard Cahn.** 174
——— **Memorial of John E. Wolff.** 182
Paragonite as a mineral species, validity of. (Schaller, Stevens). 541
Paramelaconite, a tetragonal oxide of copper. (Frondel) 657
Pawtuckaway Mts., New Hamp., petrology of. (Roy, Freedman) 202
PbO_2 and Pb_5O_8, geometrical crystallography of. (Davidson) 18
Peacock, M. A. 200, 294
Pearce, D. W. with Hanson, R. A. Colorado cerite 110
Pearl, R. M. Spessartite in pegmatite at Mt. Antero, Colo. 54
Pegau, A. A. and Bates, J. D. Some little known minerals of the Bear Mt. section of the Hudson Highlands, N.Y. 673
——— and Overstreet, W. C. Occurrence of martite in micaceous hematite near Esmont, Virginia 512
Pegmatite minerals of Striegau, Silesia, paragenesis of. (Michell) 262
Penfieldite, new analysis. (Gordon). 293
Perthite from central New Hampshire. (Smith) 203
Petrov. V. P. with Belyankin, D. C. Grossularoid group 450
Philadephia Mineralogical Society. 234, 348, 513, 630
Phillipsite 372
Pinite rock, occurrence of. (Kerr, Lomerson) 198
Plazolite 373, 450
Pleonaste 673
Pondrom, W. L. Jr., with McConnell, D. X-ray crystallography of seamanite 446

Pough, F. H. Occurrence of willemite 92
——— Formation of jarosite on pyrite ornaments............ 562
Progressive metasomatism of serpentine in the Sierra Nevada of California. (Macdonald)... 276
Pseudo heterosite=sicklerite..... 681
Pseudo palaite=hureaulite....... 682
Pseudo triplite=heterosite....... 681
Pumpellyite, zoned, from Witwatersrand, optical properties and crystallography of. (de Villiers).................... 237
Pyrite, morphology of. (Palache).. 709
Pyroaurite and sjögrenite groups, constitution and polymorphism of, (Frondel).............196, 295
Pyrochlore group, nomenclature of. (de Villiers)................ 504
Pyrope garnet vs. ruby spinel in Kansas. (Bagrowski)........ 675
Pyrophyllite (analysis)........... 400
Pyrostilpnite from Randsburg, Calif. (Murdoch)............ 130
Pyroxenes of common mafic magmas. (Hess) Part I.......... 515
——— Part II.................. 573

Quartz, rock crystal, linear thermal expansion and inversion of. (Rosenholtz, Smith)......... 103
Quartz xenocrysts in olivine basalt from southern Sierra Nevada of California. (Webb)........ 321
Quinn, A. and Stewart, G. W. Igneous rocks of the Merrymeeting Lake area of New Hampshire....................201, 633

Ramsdell, L. S................... 201
Red Lake, Ontario, granite batholith, border rocks of. (Gummer) 198
Richmond, W. E. Shortite: correction of space group.......... 629
——— **X-ray crystallography of shortite**.................... 288
Riley, L. B...................... 194
Roebling Medal, presentation to L. J. Spencer. (Winchell).... 161
——— **Acceptance of. (Spencer)**.. 163
Roedder, E. Notes on final grinding of petrographic thin-sections.. 568
Rogers, A. F.................201, 202
Rosenholtz, J. L. and Smith, D. T. Linear thermal expansion and inversion of rock crystal..... 103
——— **Linear thermal expansion of adularia**................. 391
Ross, C. S. Origin and geometric form of chalcedony-filled spherulites from Oregon..... 727
——— Sedimentary analcite..... 627
——— **with Hendricks, S. B. Chemical composition and genesis of glauconite and celadonite**..................... 683
Rowe collection. (Wilkerson)..... 507
Roy, C. J....................... 202
Rumney quadrangle, New Hampshire, igneous and metamorphic rocks of. (Page)..... 200
Ruthruff, R. F. Vermiculite and hydrobiotite................ 478

Saamite. (Volkova, Melentiev).... 135
Salvadorite=kroehnkite. (Gordon) 294
Samsonite, $Ag_4MnSb_2S_6$, unit cell and space group of. (Frondel). 25
Scapolite (mizzonite). Analysis.... ....373, 510, 674
Schaller, W. T. Bismoclite from Goldfield, Nev.............. 651
——— **and Stevens, R. E. Validity of paragonite as a mineral species**.................... 541
Seamanite, x-ray crystallography of. (McConnell, Pondrom)... 446
Sedimentary petrography. (Milner) [Book review]............. 135
Seelye, F. T. with Hutton, C. O. Composition and properties of New Zealand glauconites..... 595
Seligmannite, $CuPbAsS_3$, unit cell and space group of. (Frondel). 25
Seyrigite. (Lacroix).............. 235
Shaub, B. M. Occurrence and origin of babingtonite and other minerals from Quabbin Aqueduct, Mass............. 121
Shortite, x-ray crystallography of. (Richmond)............... 288

Shortite: correction of space group. (Richmond) 629
Sicklerite. (Mason) 681
Sjörgenite and pyroaurite groups, constitution and polymorphism of. (Frondel) 196, 295
Slawson, C. B. with Kraus, E. H. Cutting of diamonds for industrial purposes 153
——— 199
Sleight, V. G. Molybdenite at Magnet Cove, Ark 132
Smith, A. P 202, 203
Smith, D. T. with Rosenholtz, J. L. Linear thermal expansion and inversion of rock crystal 103
——— **Linear thermal expansion of adularia** 391
Sodalite, fluorescent (analysis) 443
Soda-triphylite = arrojadite 681
Spatial distribution of minor elements in single crystals. (Frondel, Newhouse, Jarrell) 197
Specimen Mt. volcanics, Rocky Mt. National Park, Colo., hydrothermal deposits in. (Wahlstrom) 551
Spencer, L. J. Acceptance of third Roebling Medal 163
Spessartite in pegmatite at Mt. Antero, Colo. (Pearl) 54
Spinel group. (Winchell) 203, 422
Stainerite = heterogenite 632
Stevens, R. E. with Schaller, W. T. Validity of paragonite as a mineral species 541
Stewart, D. Jr. Notes of some Marie Byrd Land rocks 42
——— Book review 454
Stewart, G. W. Idocrase and scapolite from Manchester, New Hampshire 509
—— **with Quinn, A. Igneous rocks of Merrymeeting Lake area of New Hampshire** 633
Stibarsen. (Wretblad) 456
Stichtite (x-ray and optical data) . . 308
Stolzite. (Palache) 429
Striegau, Silesia, pegmatite minerals. (Michell) 262
Strunz, H 631
Stutzer, O. and Noé, A. C. Geology of coal. [Book review] 232
Switzer, G. [Book review] 572
Sylvanite, atomic arrangement of. (Tunell) 457

Tamarugite. (Gordon) 235
Taylor, E. D 203
Tektites. (Barnes) 194
Tektites, moon as source of. (Nininger) 199
Tellurobismuthite. (Frondel, Peacock) 294
Thin-sections, notes on final grinding of. (Roedder) 568
Titano-lovenite (låvenite) (Kutukova) 135
Toothaker, C. R. Calcite crystals with rhomboid tubes from Guanajuato, Mexico 733
Trieuite = heterogenite 632
Tunell, G. Atomic arrangement of sylvanite 457
——— **with Fahey, J. J. Bradleyite, a new mineral** 646
Tungsten oxide, hydrous, from Oruro, Bolivia. (Kerr, Young) . 199

Ultrabasite identical with diaphorite. (Palache) 429
Unique diameters in crystallography, A. C. Gill's development of the concept of. (Burfoot) 617
Unit cell constants from 1-layerline Weissenberg pictures, check on (Wolfe) 134

Valentinite crystals from California. (Murdoch) 613
Vendendriessche, A 632
Vandiestite. (Frondel) 294
Varulite. (Mason) 681
Vermiculite and hydrobiotite. (Ruthruff) 478
Vertushkov, G. N 136
Volkova, M. I 135
Vrbaite, Tl(As, Sb)$_3$S$_5$, unit cell and space group of. (Frondel) . 25

Wahlstrom, E. E. Hydrothermal deposits in Specimen Mt. vol-

canics, Rocky Mt. National Park, Colo............... 204, 551
Webb, R. W. Quartz xenocrysts in olivine basalt from southern Sierra Nevada of California... 321
Whitlockite, a new calcium phosphate. (Frondel).......... 145, 197
Whitmore, D. R. E............. 204
Wilkerson, A. S. The Rowe Collection........................ 507
Willemite, occurrence of. (Pough). 92
Winchell, A. N. Nepheline....... 536
——— **Presentation of third Roebling Medal to L. J. Spencer**.. 161
——— **The spinel group**....... 203, 422
Wolfe, C. W. Check on unit cell constants derived from 1-layer-line Weissenberg pictures..... 134
——— **Crystallographic procedures**....................... 55
——— **Unit cell of dickinsonite**... .... 204, 338
Wolff, J. E. Memorial of. (Palache) 182
Woodford, A. O., Crippen, R. A. and Garner, K. B. Section across Commercial Quarry, Crestmore, Calif............. 351
Wretblad, P. E................ 456

Young, F...................... 199

Zincite. (Palache)............. 429
Zoisite, thulite (optical data)..... 375